DESIGN OF RECONFIGURABLE ANNULAR SLOT ANTENNA (ASA) FOR WIRELESS COMMUNICATIONS / WLAN APPLICATIONS

A Thesis
Presented to
The Academic Faculty

by

Symeon Nikolaou

In Partial Fulfillment
of the Requirements for the Degree
MASTERS OF SCIENCE IN ELECTRICAL AND COMPUTER ENGINEERING

Georgia Institute of Technology
December, 2005

DESIGN OF RECONFIGURABLE ANNULAR SLOT ANTENNA (ASA) FOR WIRELESS COMMUNICATIONS / WLAN APPLICATIONS

Approved by:

Dr. John Papapolymerou, Advisor
School of Electrical and Computer Engineering
Georgia Institute of Technology

Dr. Joy Laskar
School of Electrical and Computer Engineering
Georgia Institute of Technology

Dr. Manos M. Ttentzeris, Advisor
School of Electrical and Computer Engineering
Georgia Institute of Technology

Dr. John D. Cressler
School of Electrical and Computer Engineering
Georgia Institute of Technology

Date Approved: November 22, 2005

To ELEN
for her love, patience and support

ACKNOWLEDGEMENTS

The author wishes to acknowledge the support of the Packaging Research Center and the Georgia Electronic Design Center. In addition, the author would like to thank Prof. Manos M. Tentzeris, and Prof. John Papapolymerou for the academic supervision, Dr. George E. Ponchak, Dr. Ronglin Li, Ramanan Bairavasubramanian, Cesar Lugo, Dane Thompson, and Ileana Carrasquillo for providing assistance in theoretical justification and insight, fabrication, and measurement setup used in this research. The motivation of trying always for the best was instilled into the author's mind by his parents Niki Nikolaou and Nikolaos Nikolaou. For that the author is eternally grateful.

TABLE OF CONTENTS

Page

LIST OF TABLES

Page

LIST OF FIGURES

Page

LIST OF SYMBOLS AND ABBREVIATIONS

3-D	Three Dimensional
ASA	Annular Slot Antenna
GSM	Global System of Mobile Communications
ISM	Industrial-Scientific-Medical
MEMS	Micro-Electro-Mechanical- Systems
PIN	P-region I-region N-region
RF	Radio Frequency
WLAN	Wireless-Local-Area-Network

SUMMARY

The following document presents the design of a reconfigurable annular slot antenna (ASA) for wireless communications and wireless local area network (WLAN) applications. The multitude in different standards in cell phones and other personal mobile devices require compact multi-band antennas and smart antennas with reconfigurable features. The use of the same antenna for a number of different purposes, preferably in different frequencies is highly desirable. The proposed design demonstrates reconfigurability both in frequency and in radiation pattern. The operating frequencies are 5.2 GHz, 5.8 GHz and 6.4 GHz, and the radiation pattern is steered in three different directions with the use of shorts along the slot circumference. The use of PIN diodes is proposed to implement the switches that are used along the slot circumference, and with the matching stubs.

The annular slot antenna consists of a circular slot on a square, metal ground plane that is fed by a microstrip line, designed on the bottom of the Duroid substrate. The mean length of the slot circumference is approximately $3\lambda_s/2$ at the frequency of 5.8 GHz where λs is the equivalent wavelength in a slot line with 2 mm width, which is the design slot width. The microstrip feed line terminates in an open circuit that is approximately $\lambda_g/4$ from the ring where λ_g is the wavelength on the microstrip line. At the intersection of the microstrip line and the slot, magnetic coupling occurs, which, due to the $3\lambda_s/2$ ring circumference, creates a null in the radiation pattern in the direction of the microstrip feed line. To change the direction of the null, short circuits have to be placed on the slot. The proposed design directs the null in two additional directions forming $+45^o$ and -45^o

angles with the feeding line direction. For a non-reconfigurable design, these may be hard-wired slotline short circuits, but in the reconfigurable design, they are implemented with pin diodes. The short in the slot results in a reformation of the electric field distribution along the slot leading to a shift of the null in the short direction. The equivalent load at the input of the microstrip transmission line also changes when a short exists on the slot compared to the case when no short exists; therefore, reconfigurable matching stubs are required to keep the antenna matched at the design frequency. Linear matching stubs are also used to match the antenna at different frequencies when the slot configuration is kept constant. As a proof of concept, the antenna is designed to operate at 5.2 and 6.4 GHz in addition to the initial frequency of 5.8 GHz. To reconfigure the matching network, pin diodes are used to connect or disconnect the stubs from the microstrip transmission line and consequently shift the resonance to the desired frequency.

The proposed compact reconfigurable slot antenna may be used for IEEE802.11a (5.8GHz) WLAN and other practical wireless communications systems, such as global system of mobile communications (GSM) and Bluetooth Industrial-Scientific-Medical (ISM) devices. Research was done to obtain a basic knowledge of annular slot and reconfigurable antenna design over the past few years. Both analytical and numerical methods are used to implement a realistic, functional and efficient design. Parametric analyses using simulation tools are performed to study critical parameters that may affect the designs. Finally, the simulated designs are fabricated, and measured results are presented that validate the design approaches.

CHAPTER 1

INTRODUCTION

Antennas have been used in the past for both military and commercial applications. The original use of antennas was confined primarily in communications radio transceivers operating in the MHz range. The antennas for military applications were used for radar systems and peer to peer communications between units. Most of those antennas were bulky (Figure 1) and costly and therefore accessible to a small, specialized category of people. In the last 20 years though, personal and mobile communications networks have developed rapidly, causing an increasing need for affordable, compact and easily integrated antennas. The increasing demand for cellular phone services, wireless ınternet access, wireless cable television, among others, will force such systems to provide high throughput, and therefore very large bandwidths as well as simultaneous access to different systems through the same device, which can be accomplished with multi-band technology.

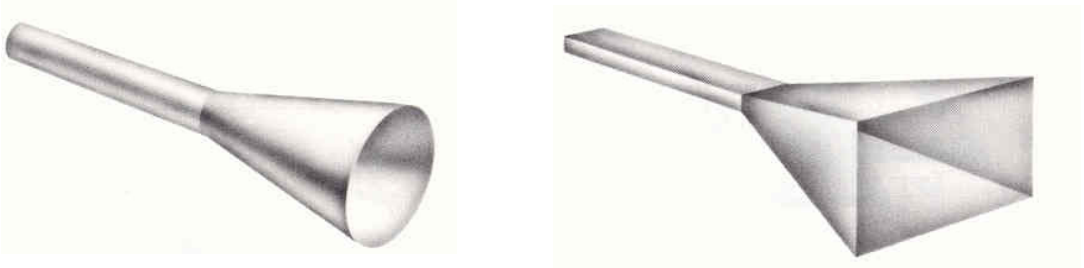

a. b.

Figure 1. (a.) circular horn, (b.) pyramidal horn.

As a result of the increasing need for gradually smaller and more affordable antennas a lot of research has been going on. The major need for commercial antennas concerns miniaturized planar antennas suitable for relatively small mobile devices like cell phones or portable computers. Patch antennas (Figure 2), printed dipoles and slot antennas fall into that category. A special type of slot antennas, annular slot antennas (Figure 3) will be the focus of this research project.

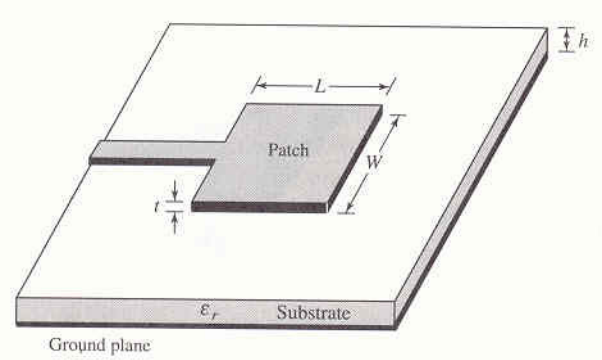

Figure 2. Patch antenna.

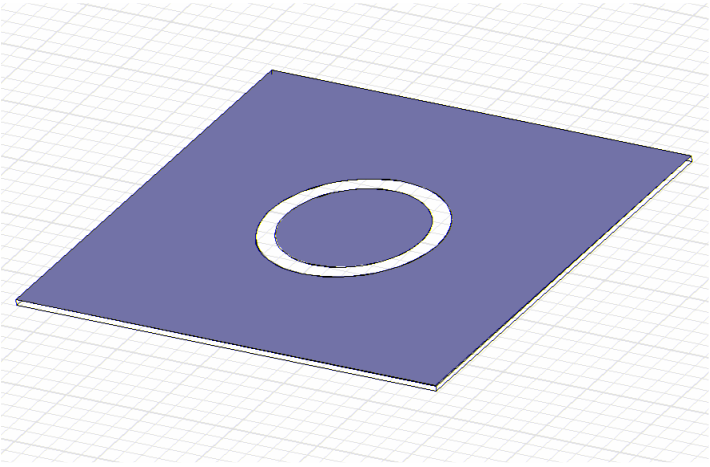

Figure 3. Annular slot antenna on dielectric material.

The need of wide operation diversity forces wireless communications systems to use different high frequency bands in the microwave and millimeter wave regions; frequency bands in which slot antennas are often used. However, slot antennas have limited bandwidth problems and not many bandwidth control techniques have been published. An additional problem is the existence of many mobile users who probably use the same operation frequency. Therefore their signal becomes an undesired interferer for a neighboring user. So a technique is needed to potentially reject the interference from a certain direction. If the blockage of such a signal is impossible then the interested user has to immune his receiver to the received signal. This can be done by directing a radiation pattern null in that direction and consequently blinding the receiver in that direction. This can be done using a reconfigurable radiation pattern antenna that enables the user to turn the radiation pattern in the desired direction in a similar concept that radar phased arrays direct the narrow main beam to an electronically controlled direction.

Apparently the need for a reconfigurable radiation pattern antenna and a multi frequency antenna is obvious. An antenna design with a combination of those two reconfigurability characteristics would be highly desired. This research focuses on a technique to control the radiation pattern and at the same time maintain a multi frequency operation for a single low profile, low cost antenna. An annular slot antenna loaded with PIN diodes along its circumference is proposed for this purpose. The planar antenna is fabricated on one side of a Duroid substrate and the microstrip feeding line with the matching network is fabricated on the opposite side of the board. The central frequency is 5.8 GHz and, by reconfiguring the matching circuit, the antenna was also designed to operate at 5.2 GHz and 6.4 GHz. Pin diodes are also used to short the ASA in pre-

selected positions along the circumference, thereby changing the direction of the null in the plane defined by the circular slot changes. As a proof of concept, two pin diodes are placed 45 º on both sides of the feeding line along the ASA and the direction of the null is shown to align with the direction defined by the circular slot center and the diode. Consequently a design that is reconfigurable in both frequency and radiation pattern is accomplished. The antenna was designed using Ansoft HFSS simulator and was fabricated in Georgia Tech facilities. The fabricated prototypes were tested and measured and their results are compared with the simulated results. Return loss and radiation pattern measurements and simulations are presented, which are in very good agreement.

Basic theory about slot antennas and annular slot antennas is presented in Chapter 2 along with the approaches followed by other people and reported in literature. In Chapter 3 the frequency reconfigurable design, the design and optimization of linear matching stubs and their integration with PIN diodes are discussed. The radiation pattern reconfigurable design and an accurate model that discusses the null rotation are presented in Chapter 4. Finally, Chapter 5 presents conclusions and potential applications for the proposed antenna design.

CHAPTER 2

BACKGROUND

The slot antennas have the advantage of being able to produce bidirectional radiation patterns with higher bandwidth, compared to patch antennas. In addition antennas with desired polarization can be produced by using a combination of strip conductors and slots arranged along the sides of a mictrostrip feed. The operation principles and the antenna characteristics of slot antennas are shortly discussed in this chapter. The basic element of the rectangular slot is presented at first, and the issues evolved from the microstip feeding are presented. Based on the concepts already discussed about the microstrip fed rectangular slot, the microstrip fed annular slot and the loaded annular slot are introduced. In the second section, the work done by other people on multi band and reconfigurable slot antennas is noted. Finally some information about pin diodes which implement the switches for the reconfigurable antenna is provided.

2.1 MICROSTRIP-FED RECTANGULAR AND ANNULAR SLOT ANTENNAS

2.1.1 RECTANGULAR SLOT

A microstrip slot antenna comprises a slot cut in the ground plane of the micostrip line such that the slot is perpendicular to the strip conductor of the microstrip line. The slot is excited by the fields of the microstrip line. For efficient excitation of the slot, the strip conductor is terminated in an open-circuited stub beyond the edge of the slot as shown in Figure 4. Alternatively the strip conductor can be short-circuited

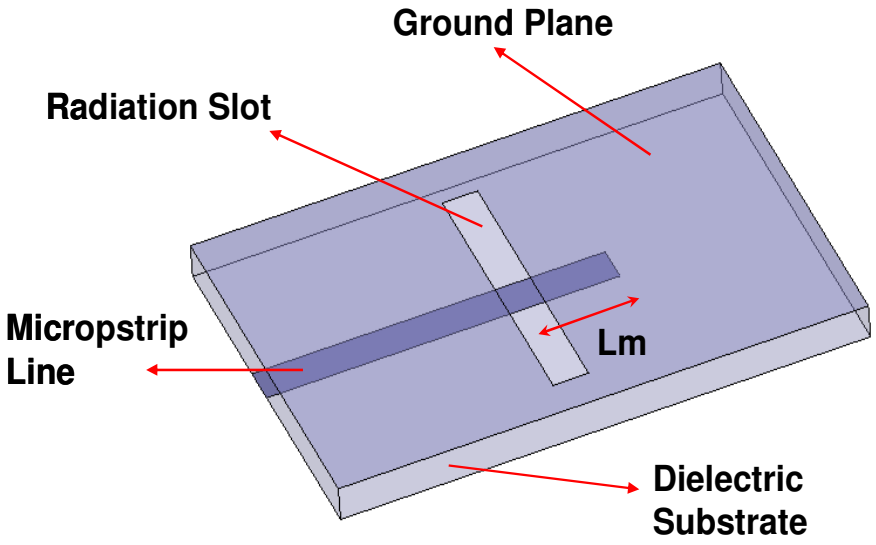

Figure 4. Microstrip fed rectangular slot antenna

through the dielectric substrate to the edge of the slot but this second technique is more difficult to fabricate. The length Lm of the open-circuited microstrip stub is approximately a quarter wavelength long so that an effective short circuit is realized at the outer edge of the slot as shown in Figure 4. A center-fed slot antenna has a very high radiation resistance, therefore in order to match the antenna to the characteristic impedance of the microstrip line a matching network needs to be used.

There are three ways to reduce the resistance seen by the feed line for a given slot size. The first is off-center feeding as suggested in [1]. The second is stub tuning as suggested by Pozar in [2]. This technique is similar to the technique in Figure 4 except that the length Lm of the microstrip stub is longer than a quarter wavelength. The stub tuning introduces a reactive loading on the antenna that changes the resonant frequency. The stub is designed so that the input resistance compares with the feed line impedance at the new resonance frequency. The third feeding option is that the slot is center fed but

forms an angle with the feed slot. Consequently the slot is not perpendicular to the feed line. The slot antenna has the advantage of low cross-polarization as compared to the microstrip patch antennas [3]. It is normally bidirectional but can become unidirectional by using a metallic cavity or a metallic reflector in the back side. The microstrip-fed has been studied by many researchers both theoretically and experimentally. Some approximate network models have also been proposed to design the antenna efficiently. For additional information the reader can refer to [4].

The rectangular slots are considered to be the dual equivalent to linear wire dipoles. The radiation patterns in E and H plane for s rectangular slot with length L_s and width $W_s << \lambda_o$ where the E field distribution along the slot is given by $E_y = E_o\left(\cos \pi x / L_s\right)$ are obtained as follows:

E plane ($\varphi=\pi/2$) : $E_\phi = 0$, and $E_\theta = \dfrac{jk_o}{2\pi^2}\dfrac{e^{-jk_o r}}{r} E_o W_s L_s$ (Omni-directional)

H plane ($\varphi=0$) : $E_\theta = 0$, and $E_\phi = \dfrac{jk_o}{2\pi^2}\dfrac{e^{-jk_o r}}{r} E_o W_s L_s \cos\theta \dfrac{\cos k_o L_s \sin\theta/2}{\left(k_o L_s \sin\theta/\pi\right)^2 - 1}$

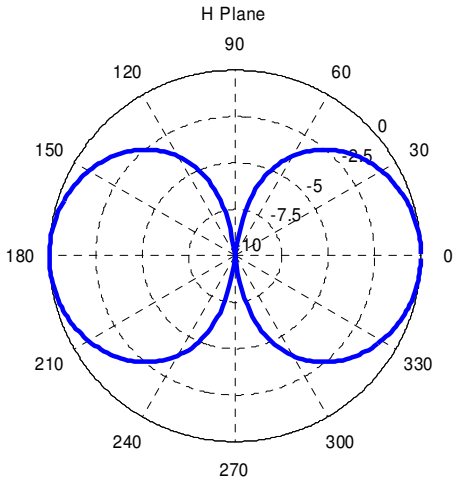

Figure 5. H Plane E_φ polarization for $Ls=\lambda_o/2$

2.1.2 ANNULAR SLOT

The annular slot antenna is a variation of the rectangular loop antenna that consists of 4 linear rectangular slots in a rectangle orientation. An annular slot antenna comprises a circular slot in the ground plane of a dielectric substrate, fed by a microstrip conductor as shown in Figure 6. This kind of antenna has possible application in vehicular antenna for mobile communications, since it can radiate power in low elevation angles [5]. In urban mobile communications, incident waves to mobile stations come mostly from directions having low elevation angles, about 30^o up from the horizontal plane. Radiation pattern analysis of an annular slot antenna is presented next

Consider the geometry of an annular slot in the coordinate system of Figure 6. An annular slot in an infinite conducting plane can be viewed as an annular distribution of the magnetic current given by $\vec{M}(\rho,\phi') = \vec{E}_a(\rho,\phi') \times \hat{n}$ where $\vec{E}_\alpha$ is the aperture electric field and $\hat{n}$ is the unit vector normal to the aperture. The far field radiation patterns of an annular slot antenna can be evaluated by using the vector electric potential method. From the vector electric potential the far field components E_θ end E_φ can be written as:

$$E_\theta = \frac{-jk_o}{4\pi}\frac{e^{-jk_o r}}{r}\int_0^{2\pi}\int_\alpha^{\alpha+Ws}\{M(\rho)\sin(\phi'-\phi)+M(\phi')\cos(\phi'-\phi)\} \times \exp\left(j\rho k_o \sin\theta\cos(\phi-\phi')\right)\rho d\rho d\phi'$$

$$E_\phi = \frac{-jk_o}{4\pi}\frac{e^{-jk_o r}}{r}\cos\theta\int_0^{2\pi}\int_\alpha^{\alpha+Ws}\{M(\rho)\cos(\phi'-\phi)-M(\phi')\sin(\phi'-\phi)\} \times \exp\left(j\rho k_o \sin\theta\cos(\phi'-\phi)\right)\rho d\rho d\phi'$$

where α is the inner radius of the slot and Ws the slot width.

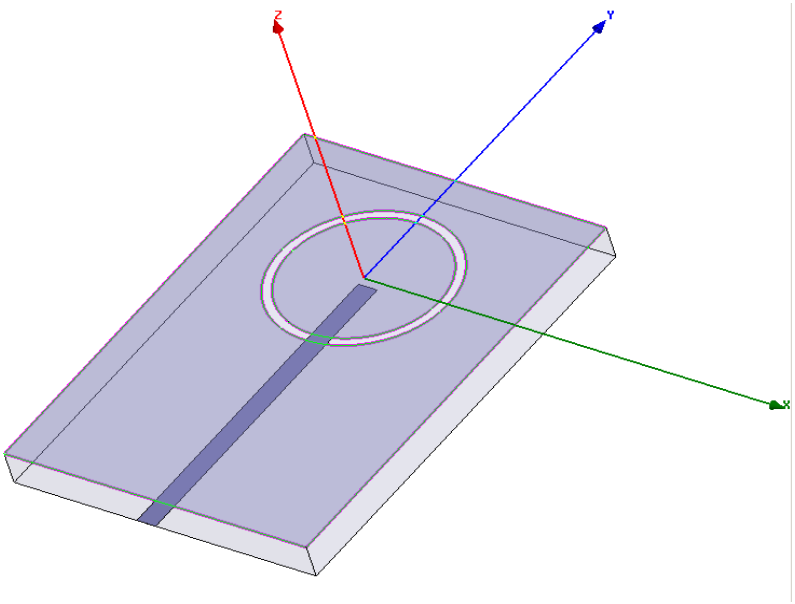

Figure 6. Microstrip fed annular slot

$$\vec{M}(\rho,\phi') = \vec{M}(\rho)\hat{\rho} + \vec{M}(\phi')\hat{\phi} = -\vec{E}_{\phi}\hat{\rho} + \vec{E}_{\rho}\hat{\phi}$$

E_ρ and E_φ are the slot field components in the ρ and φ directions, respectively. When the slot width $W_s << \lambda_o$ is small enough one can assume that $E_\varphi = 0$. With this assumption and after the integration with respect to φ the electric far field expressions become:

$$E_\theta = -j^n E_o \alpha \frac{k_o W_s}{2} \frac{e^{-jk_o r}}{r} \cos n\phi J_n'(ak_o \sin\theta)$$

$$E_\phi = j^n n E_o \frac{W_s}{2} \frac{e^{-jk_o r}}{r} \sin n\phi \cot\theta J_n(ak_o \sin\theta)$$

J_n and J_n' are the Bessel function of order n and it's derivative respectively. The plots of E field in planes E and H, when n=0 and n=1 are presented in Figures 7-9.

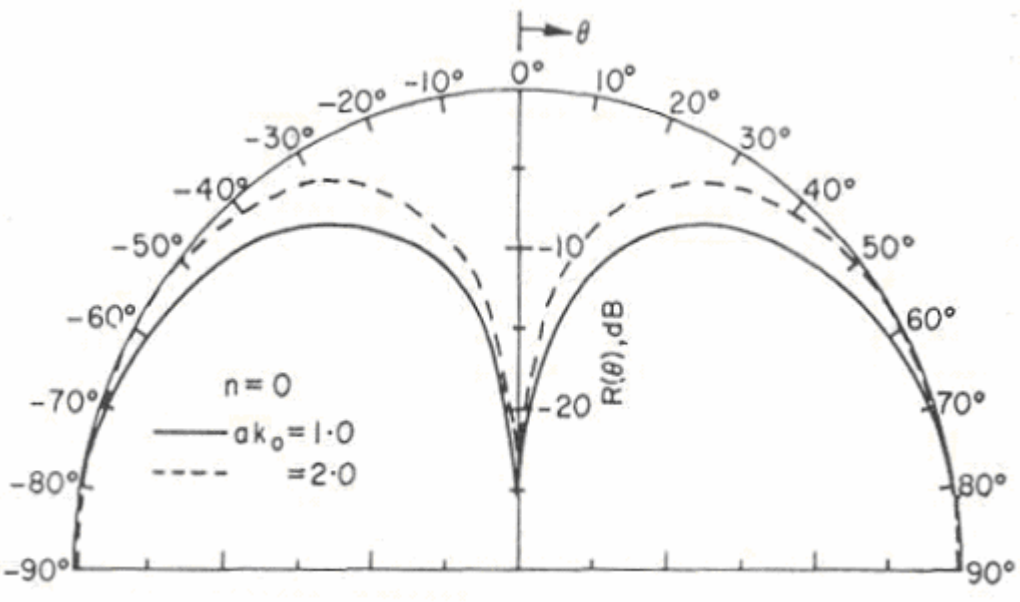

Figure 7. Radiation patterns of annular slots when n=0 and $W_s << \lambda_o$ [4]

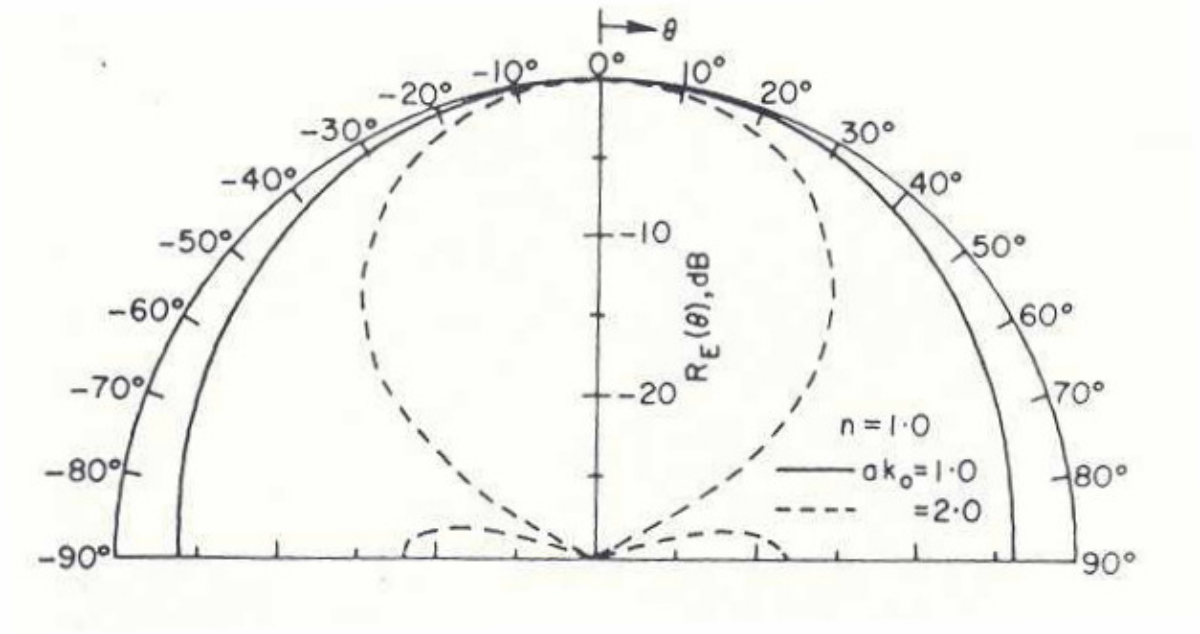

Figure 8 Eplane radiation patterns of annular slots when n=1 and $W_s << \lambda_o$ [4]

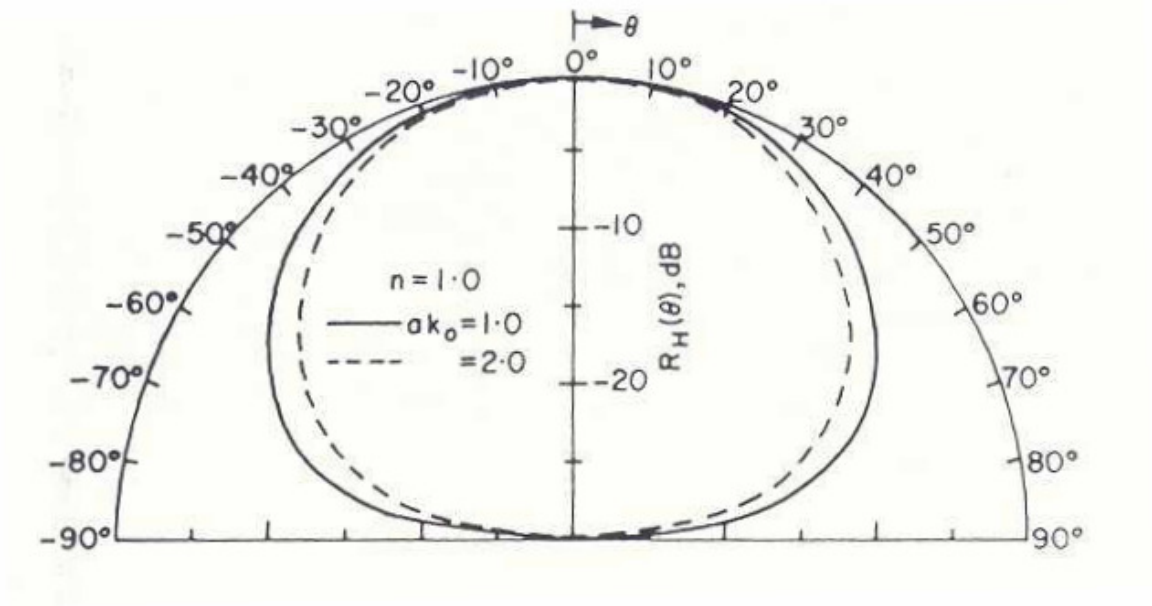

Figure 9. E plane radiation patterns of annular slots when n=1 and $W_s << \lambda_o$ [4]

Circular polarization can be realized by feeding it such that two modes with orthogonal polarizations, equal amplitude, and 90^o phase difference are excited. For this purpose one can choose between a single feed design with a power splitter and a dual feed design. Circular polarization can be achieved by loading the slot with a short along the circular circumference. The loaded antenna has been studied by Morishita et al. [5]. The antenna characteristics such as input impedance, resonance frequency, bandwidth, radiation pattern and polarization have been studied as a function of the position of the short in the slot aperture. It has been shown that the resonant frequency can be varied by changing the shorting position. Additionally the radiation patterns can be varied.

2.2 PAST TECHNIQUES AND APPROACHES

The multitude of different standards in cell phones and other personal mobile devices require compact multi-band antennas and smart antennas with reconfigurable features. The use of the same antenna for a number of different purposes, preferably in different frequencies is highly desirable. A number of different reconfigurable antennas, planar and 3-D have been developed. Some of them were developed for radar applications [6]-[7] and other planar antennas were designed for wireless devices [8]-[9]. Reconfigurable patch antennas were also designed to operate in both L and X bands [10]. Most of those papers demonstrate only frequency reconfigurability. The reconfigurable Annular Slot Antenna (ASA) proposed for this project operates at three frequencies with the central frequency at 5.8 GHz, and it also has a reconfigurable radiation pattern. It will be fabricated on low cost material and is a compact design suitable for integrating in mobile systems. The annular slot antenna on dielectric material has been described explicitly in [5]. The effect of one shorted point along the circumference has been explored in [7], and an application of a shorted ASA integrated with a narrowband filter is presented in [12], while the effect of capacitive loading is investigated in [13]. While the literature concerning the shorted ASA is limited, a significant number of papers have been published investigating feeding techniques and several antenna features like the input impedance, the radiation efficiency, and the radiation pattern of a pure ASA. For the antenna feature analysis, both analytical [14], [15] and numerical techniques [16] were used and different approaches or models were applied [17]. Various feeding lines [18] and feeding techniques are used in order to achieve broader bandwidth, or to demonstrate multi-band operation [19] – [24]. In these designs all resonating frequencies

are excited simultaneously.

The design proposed by [20] (Figure 10) uses an asymmetric microstrip feeding that crosses the slot at two points to support multiple resonances. The resonances created are 3.5 GHz, 4.5 GHz and 6.4 GHz and are excited simultaneously. The slot antenna is fabricated on low ε_r material (ε_r=2.45) and the dielectric thickness is 0.762 mm. Although the antenna has three resonances, interference between them cannot be treated because all three resonances co-exist.

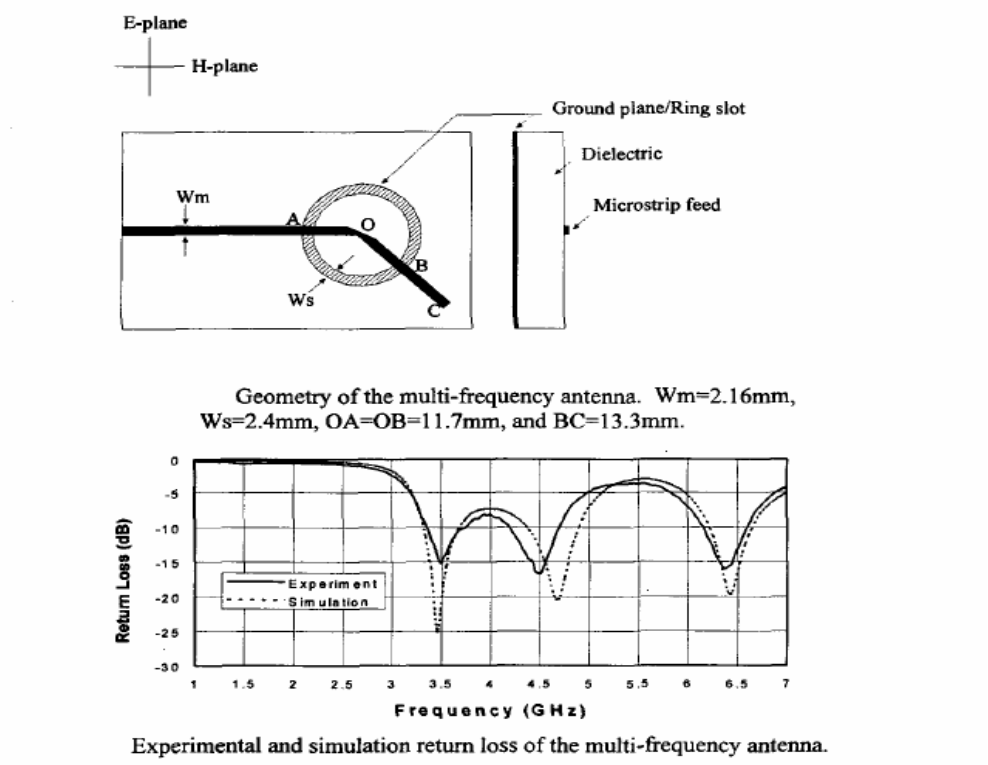

Figure 10. Multi-frequency annular slot antenna [20]

A different multi-band antenna proposed in [21] (Figure 11) has a different design approach. A simple microstrip feeding is used but there is a second slot inside the first annular slot that creates a different resonance. In this design all frequencies ranging from 2.4 GHz up to 6.8 GHz are excited at the same time.

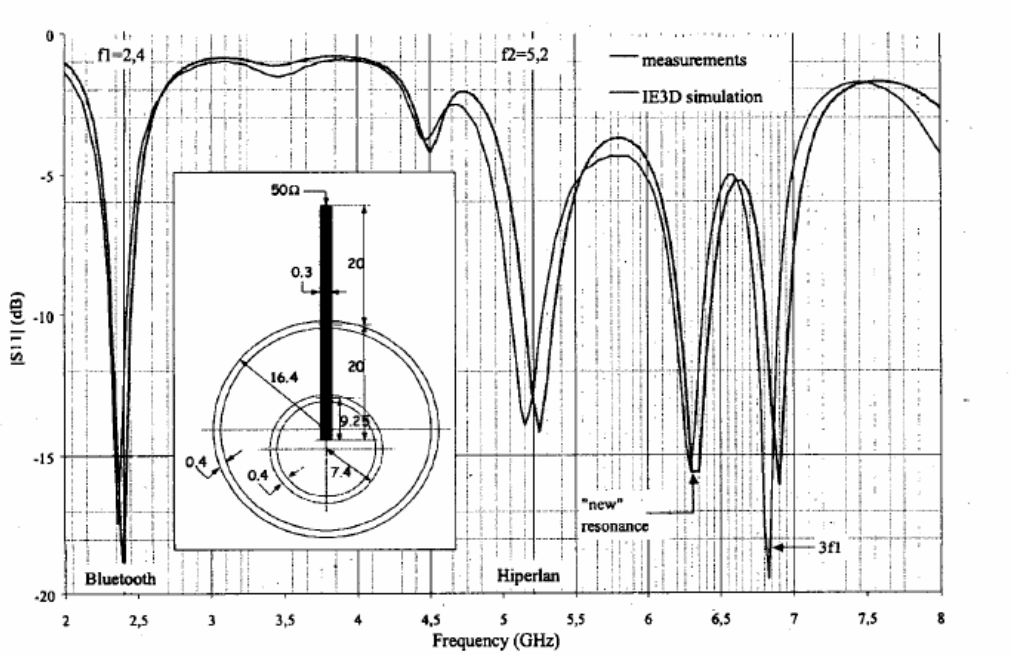

Return loss of the dualband antenna.

Figure 11. Multi-band annular slot antenna [21]

A similar design proposed by N. Behdad and K. Sarabandi in [24] (Figure 12) consists of a semi-circular slot. The design principle is the same as the one used for the previous design, the added "diameter" creates a second resonance but in this case the antenna becomes a broadband antenna since the S_{11} parameter between the two resonances remains below -10 dB, therefore it radiates in the whole range. In that case also the resonances co-exist. In the design proposed in this project an attempt is made to create an antenna with multi-resonances which are excited independently to one another.

Peroulis in [25] has presented a reconfigurable rectangular slot antenna using pin diodes. The proposed design was reconfigurable only in frequency.

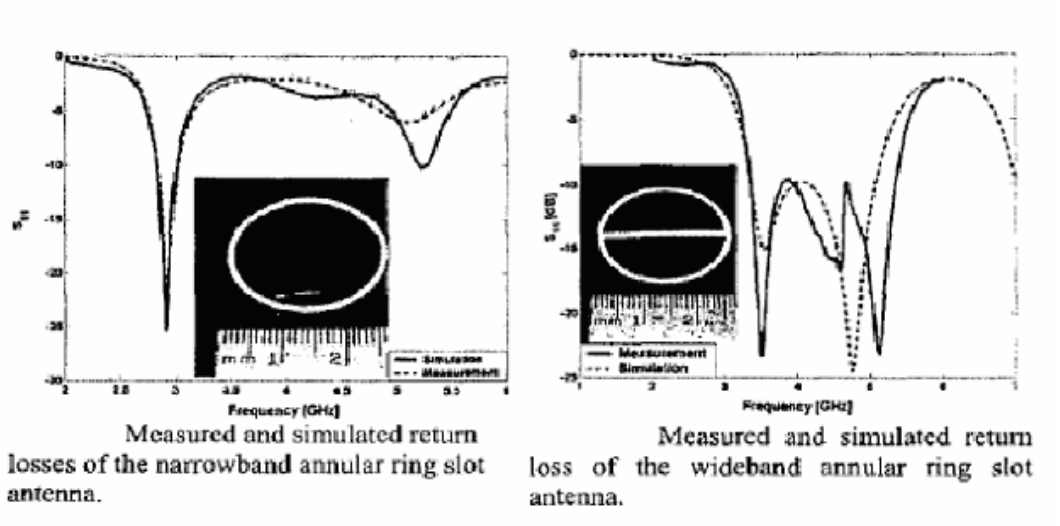

Measured and simulated return losses of the narrowband annular ring slot antenna.

Measured and simulated return loss of the wideband annular ring slot antenna.

Figure 12. Semi-circular slot antenna [24]

While the radiation pattern is an essential parameter of an antenna, very little has been published about radiation pattern control techniques for the ASA [26].

In this project, we present for first time an annular slot antenna with simultaneous frequency and radiation pattern reconfigurability, by using pin diodes to short the ASA at pre-determined locations, and to reconfigure the matching circuit. For this antenna only one frequency resonates at a time, which is desirable when there are power or interference issues.

2.3 PIN DIODES

A PIN diode is a semiconductor device that operates as a variable resistor at RF and microwave frequencies. The resistance value of the PIN diode is determined only by the forward biased dc current. In switch and attenuator applications, the PIN diode should ideally control the RF signal level without introducing distortion which might change the shape of the RF signal. An important additional feature of the PIN diode is its ability to

control large RF signals while using much smaller levels of dc excitation. A model of a PIN diode chip is shown in Figure 13. The chip is prepared by starting with a wafer of almost intrinsically pure silicon, having high resistivity and long lifetime. A P-region is then diffused into one diode surface and an N-region is diffused into the other surface. The resulting intrinsic or I-region thickness (W) is a function of the thickness of the original silicon wafer, while the area of the chip (A) depends upon how many small sections are defined from the original wafer. The performance of the PIN diode primarily depends on chip geometry and the nature of the semiconductor material in the finished diode, particularly in the I-region.

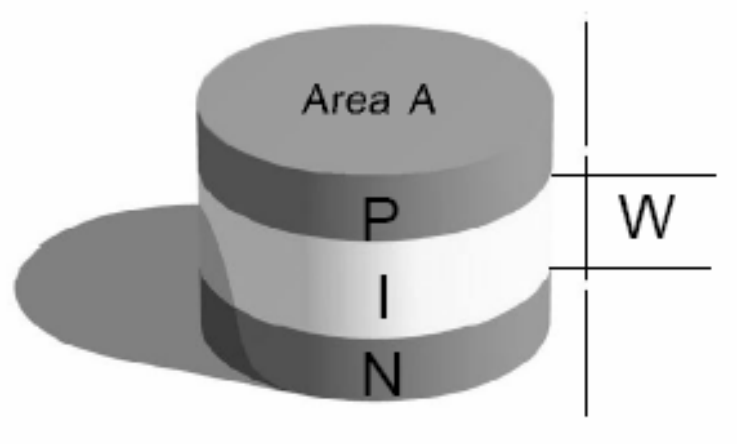

Figure 13. PIN diode schematic

2.3.1 FORWARD BIASED PIN DIODES

When a PIN diode is forward biased, holes and electrons are injected from the P and N regions into the I-region. These charges do not recombine immediately. Instead, a finite quantity of charge always remains stored and results in a lowering of the resistivity

of the I-region. The quantity of stored charge, Q, depends on the recombination time, τ (the carrier lifetime), and the forward bias current, I_F, as follows:

$Q = I_f \tau$ *[Coulomb]* The resistance of the I-region under forward bias, Rs is inversely proportional to Q and may be expressed as $R_S = \frac{W^2}{(\mu_N + \mu_P)Q}$ *[Ohms]* where: W = I-region width, μ_N = electron mobility, μ_P = hole mobility

Combining those equations, the expression for R_S as an inverse function of current is shown as $R_S = \frac{W^2}{(\mu_N + \mu_P)Q\mathrm{I}_f \tau}$. This equation is independent of area. In the real world the R_S is slightly dependent upon area because the effective lifetime varies with area and thickness due to edge recombination effects.

2.3.2 REVERSE BIASED PIN DIODES

At high RF frequencies when a PIN diode is at zero or reverse bias, it appears as a parallel plate capacitor, essentially independent of reverse voltage, having a value of: $C = \frac{\varepsilon \mathrm{A}}{W}$ *[Farads]* where: ε = silicon dielectric constant, A = junction area W = I-region thickness. The lowest frequencies at which this effect begins to predominate are related to the dielectric relaxation frequency of the I-region, *f*t, which may be computed: $f_\tau = \frac{\mathrm{I}}{2\pi\rho\varepsilon}$ where: ρ = I-region resistivity.

At frequencies much lower than f_τ the capacitance characteristic of the PIN diode resembles a varactor diode. Because of the frequency limitations of common test equipment, capacitance measurements are generally made at 1 MHz. At this frequency the total capacitance, C_T, is determined by applying a sufficiently large reverse voltage

which fully depletes the I-region of carriers. Associated with the diode capacitance is a parallel resistance, Rp, which represents the net dissipative resistance in the reverse biased diode. At low reverse voltages, the finite resistivity of the I-region results in a lossy I-region capacitance. As the reverse voltage is increased, carriers are depleted from the I-region resulting in an essentially lossless silicon capacitor. The reverse parallel resistance of the PIN diode, Rp, is also affected by any series resistance in the semiconductor or diode contacts. The equivalent circuits are presented in Figure 14. C_T is the total capacitance and L is the total package inductance.

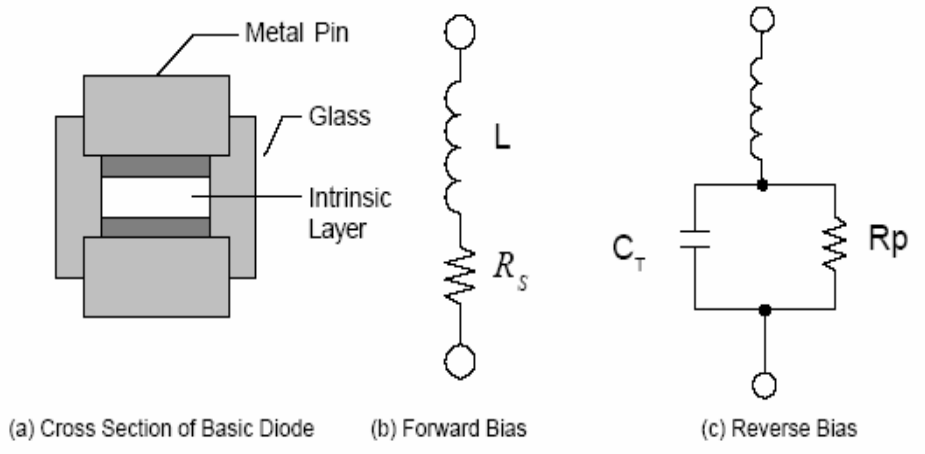

Figure 14. Equivalent circuits for reverse and forward biased diode

2.4 SUMMARY

In this chapter, the necessary theoretical background to comprehend the design parameters of the proposed reconfigurable ASA, has been presented. The radiation and matching principles of rectangular and annular slots have been briefly discussed and the suggested designs and applications by other researchers have been outlined. Finally the

model and the equivalent circuits for the pin diode have been mentioned. The principles discussed here will be implemented for the design and fabrication of a reconfigurable in both frequency and radiation pattern ASA.

CHAPTER 3

FREQUENCY RECONFIGURABLE DESIGN

The annular slot antenna has been shown to demonstrate high radiation efficiency in a wide range of frequencies. In several examples demonstrated in the previous chapter the microstrip fed annular slot has presented multi frequency behavior. The drawback in those designs is that the radiating resonances appear simultaneously and in indigenous non pre-selected frequencies. An example would be a harmonic resonance that appears as a result of the structure and not as a result of a design methodology. In this chapter the use of linear matching stubs is proposed to match the antenna in pre-selected frequencies. The matching stubs are connected to the microstrip feeding line using PIN diodes as switches.

3.1 ANTENNA STRUCTURE

The annular slot antenna consists of a circular slot on a square, metal ground plane that is fed by a microstrip line fabricated on the opposite side of the substrate as can be seen in Figure 15. The design parameters are summarized in Table 1. The mean length of the slot circumference is approximately $3\lambda_s/2$ at the design frequency where λ_s is the equivalent wavelength in a slot transmission line with slot width w=R-r, which is small compared to λ_s. The microstrip feed line terminates in an open circuit that is approximately $\lambda_g/4$ from the ring where λ_g is the guided wavelength on the microstrip line. At the intersection of the microstrip line and the slot, magnetic coupling occurs, which, due to the $3\lambda_s/2$ ring circumference, creates a null in the radiation pattern in the direction of the microstrip feed line. The 3-D pattern is presented in Figure 16 and the 2-D Eφ polarization is presented in Figure 17.

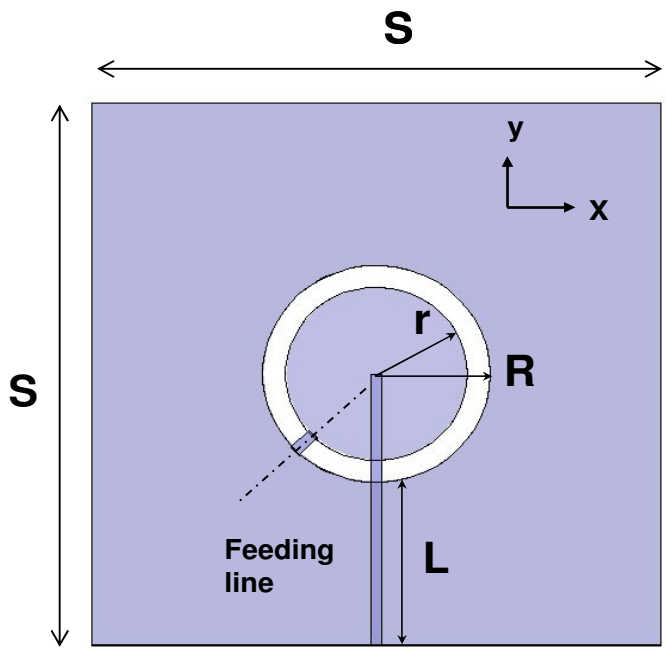

Figure 15 ASA front side. The feeding line is on the back side of the board

In Figure 15 and all subsequent figures x-y axes are used. The x axis corresponds to φ=0º and the y axis to the φ=90º. The radiation patterns and all references on angle positions are consistent with the aforementioned notation.

TABLE I
Antenna structure dimensions

Symbol	Value in mm
S	50
L	15
R	10
r	8

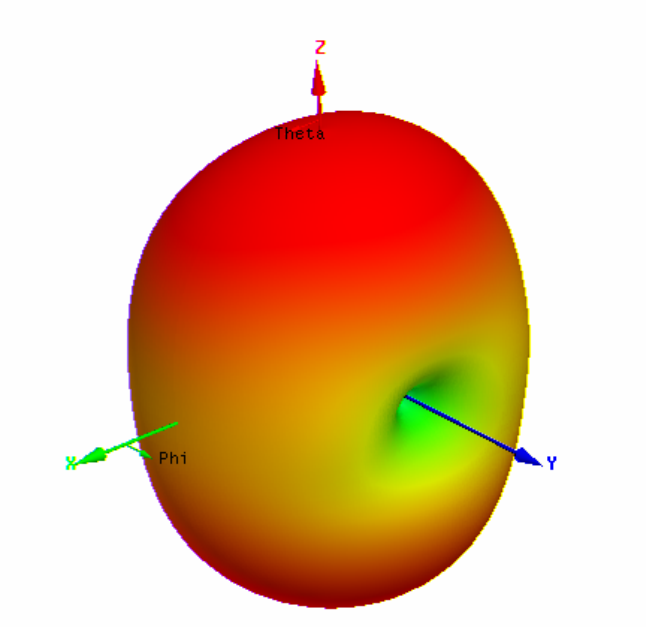

Figure 16. 3-D Radiation pattern of ASA without short along the circumference The null is directed in the feeding line direction. (y- axis)

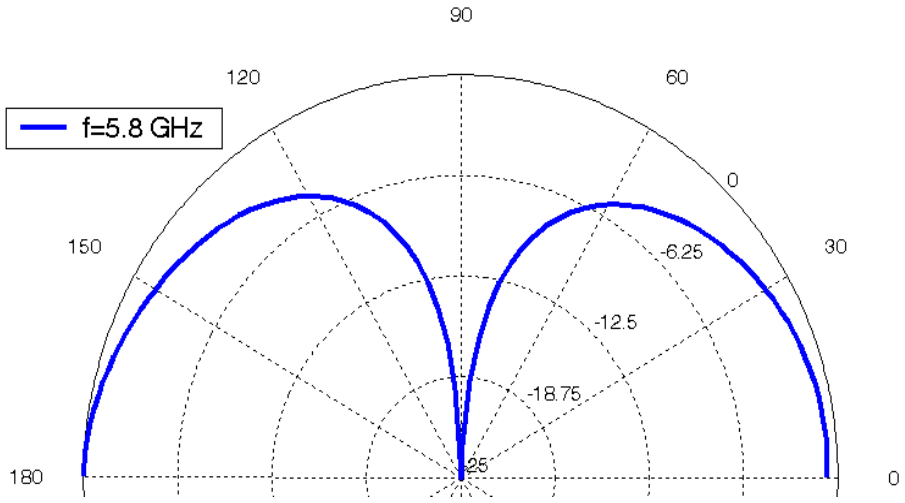

Figure 17. Eφ radiation pattern at 5.8 GHz for ASA without short

The shorted slot is printed on the front side, and the feeding line with the matching stubs, are printed on the back side of the board, using standard photolithography. The antenna is fabricated on a 50 mm x 50 mm, 635 μm thick, low loss (tanδ=0.0025) Rogers RO3006 with ε_r=6.15 and a copper thickness of 18 μm. The antenna is fed by a 50 Ω microstrip line with width of 0.92 mm and the matching stubs are also 0.92 mm wide. The slot has an outer radius R=10 mm and inner radius 8 mm resulting a slot width of 2 mm. The feeding line is 25 mm long and the end of the line is at the slot center.

3.2 DESIGN METHODOLOGY

The ASA using various feeding techniques has been shown to have a relatively wide bandwidth compared to a patch or other narrowband antennas [27]-[28]. For the design dimensions used in this project, simulations predict radiation efficiency greater than 80% over the frequency range from 4.8 GHz to 6.5 GHz. Since the radiating element can radiate over a wide range, the matching network must also support a broad bandwidth. Moreover, the use of diodes to create shorts in the annular ring for null reconfiguration also affects the input impedance, and this also must be accounted for in the matching circuit. The following technique was experimentally tested for the shorted ASA. Instead of a broadband matching network, a reconfigurable matching network employing stub tuners was designed to support three narrowband frequency ranges. At the center frequency of 5.8 GHz, the input admittance was determined from the simulations, and this admittance was transferred along the 50 Ω microstrip line to the point where the admittance had a real part of 0.02 siemens (=1/50 siemens) and a random imaginary part. At that point, an open circuit microstrip stub was placed parallel to the

transmission line to cancel the imaginary part. For the case under study with the hard-wired short at 45^{o} the required stub to match the ASA should be put 7.23 mm far from the board edge and should have length equal to 4.21 mm (Figure 18). For the calculation of the exact position and length of the matching stubs a code in Matlab was deeloped. For the other frequencies, the impedance at the port needs to be determined with the first matching stub in place so the other two frequencies are matched using the combination of two stubs for each one of them. That means that with stub L2 connected to the microstrip line, the new impedance at the port is used to define the position (D1=5.49mm) of the second stub L1=4.98 mm to match the ASA at 5.2 GHz. Those additional stubs have been shown not to affect in any way the radiation pattern. For the experimentally tested case the short on the slot is placed at 45º from the feeding line, namely at 225^{o} as can be seen in Figure 19. Because of symmetry, the same matching stubs can be used when the short is placed at the symmetrical position 45º towards the opposite direction, which is at 315^{o}.

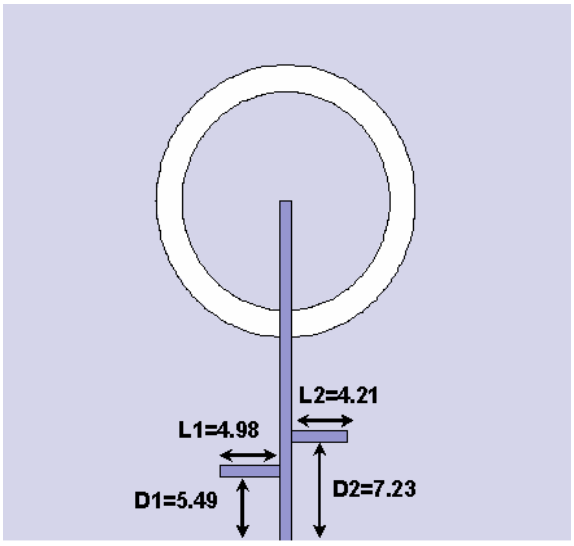

Figure 18. ASA matched at 5.2 GHz with 2 hard-wire stubs

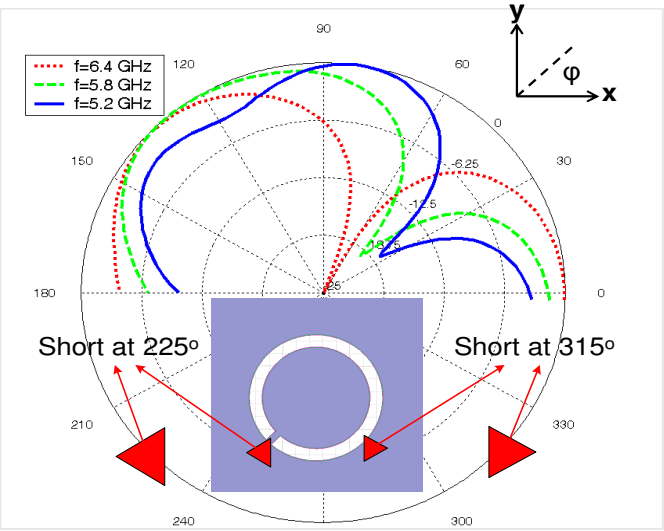

Figure 19. Simulated normalized radiation patterns on the x-y plane with a short circuit at 225°. The null direction for the slot without any short would be in the 90° direction with respect to the plot labeling.

In order to match the ASA at 6.4 GHz L1 and D1 should be 3.22 mm and 4.10 mm respectively. The resulted, simulated return loss plots for those three cases are shown in Figure 20.

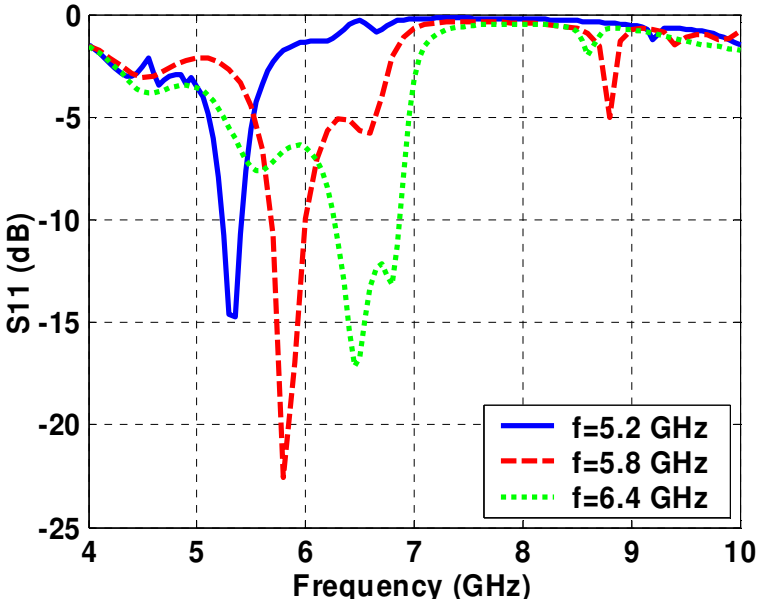

Figure 20. Simulated return loss with linear matching stubs

The definition of the stubs length and position would be adequate if we wanted to create three different antennas, one for each frequency since they seem to be matched well as can be seen in Figure 20 from the three radiating resonances (below -10 dB) . However in order to create a single reconfigurable design some additional tuning is necessary. DC bias lines need to be added on the feeding line in order to provide a DC path to forward and reverse bias the PIN diodes that are used. Although the bias lines are very thin in order to be very resistive to the RF signal there is still some leakage that has to be taken into consideration in order not to compensate the accuracy. Consequently the aforementioned matching technique has to be repeated for a design than includes all three stubs and the necessary bias lines (Figure 21).

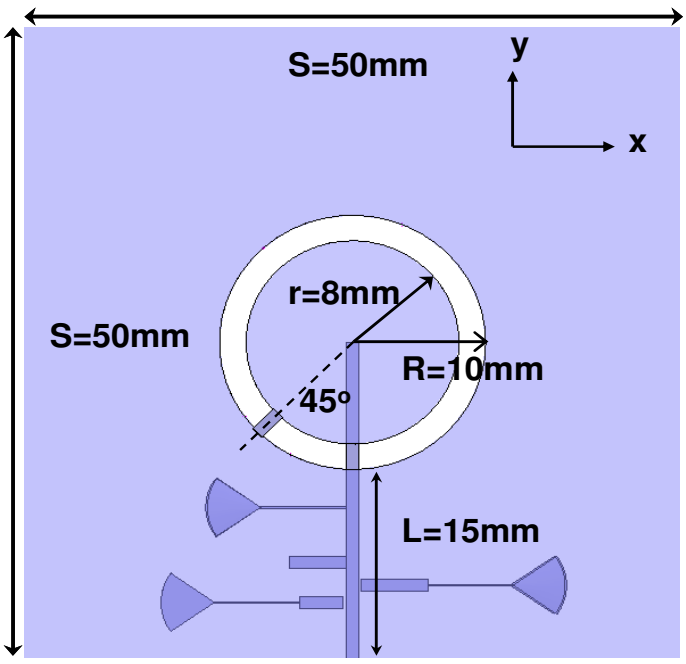

Figure 21 Annular Slot Antenna schematic The feeding line with the matching stubs are on the bottom and the annular slot antenna is on the top side of the substrate. The short is placed at φ=225°, else 45° far from the feeding line

The diodes to be used are small compare to the stub width (0.92 mm) and as a result a tapered segment is necessary in order to "match" the linear stub to the 200 µm wide ASI 8001 PIN diodes. Therefore the length of the stubs needs to be redesigned in order to meet the diode interface needs. The stubs schematic without the tapered segments is presented in Figure 22. The stubs' lengths for f=5.2 GHz and f= 6.4 GHz are L'1=4.98 mm and L'2=3.22 mm respectively.

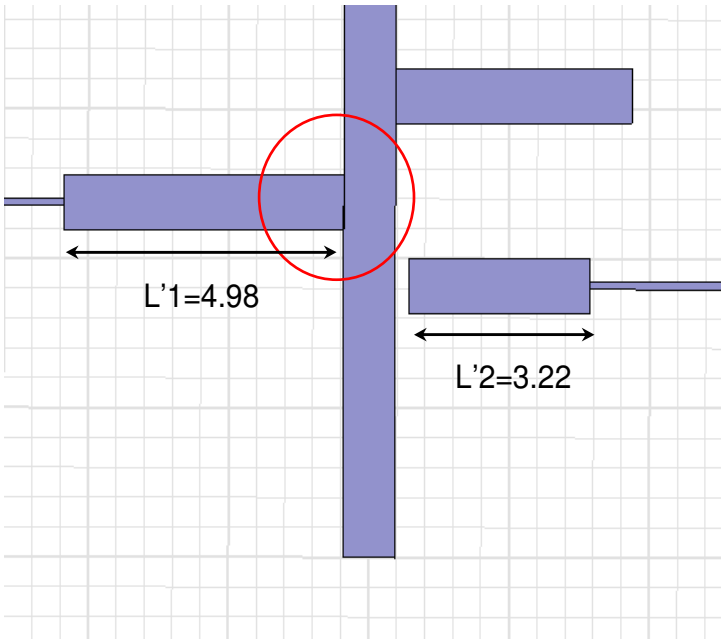

Figure 22. Linear matching stubs without tapered segment.

The addition of the tapered segments reduces the linear segment's length. The diodes are simulated as a perfect conductor with dimensions 200 µm x 200 µm. The linear segment is simulated with Momentum ADS as a single port circuit and it's characteristic S11 is set as the goal for an equivalent stub (Figure 23) constituted from a small square part (diode equivalent) the linear tapered part, and a linear part with a variable to be optimized length. The linear part is 0.92 mm wide on the linear stub side and 200 µm wide on the

diode side. The optimized dimensions for the linear parts are L1=3.45 mm for the 5.2 GHz stub and

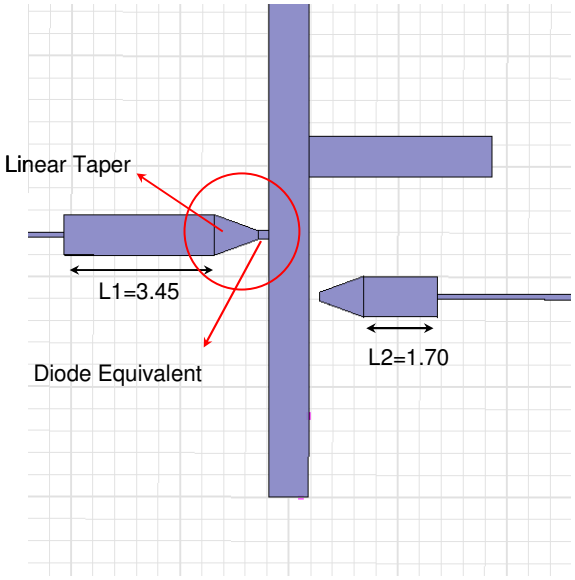

Figure 23. Matching stubs with tapered segments

L2=1.70 mm for the 6.4 GHz stub. A photograph of the fabricated prototype that shows the soldered diodes on the taperd stubs is presented in Figure 24. The used ASI 8001 PIN diodes will be referred to as “small” diodes.

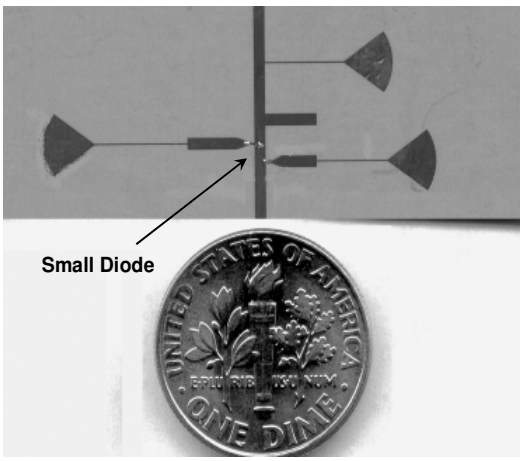

Figure 24. Photograph of the back side of the frequency reconfigurable design. Two ASI 8001 PIN diodes are observed connecting the matching stubs to the feeding line. The dc bias lines are also visible.

3.3 FREQUENCY RECONFIGURABLE DESIGN VALIDATION

In order to investigate the effect of the diodes, three different designs with the correct matching network hard wired for each of the three frequencies were tested. Simulations and measurements are in good agreement, (Figure 25) with a small shift downwards for the 6.4 GHz resonance, which could be a result of fabrication inaccuracy and imperfect connector soldering. In addition to the "small" diodes used for the matching stubs two more MBP-1035-E28 PIN diodes are used to implement the switches on the slot circumference. The MBP-1035-E28 PIN diodes will be referred to as "big" diodes. The front side of the reconfigurable design with the diodes soldered on the slot is presented in Figure 26.

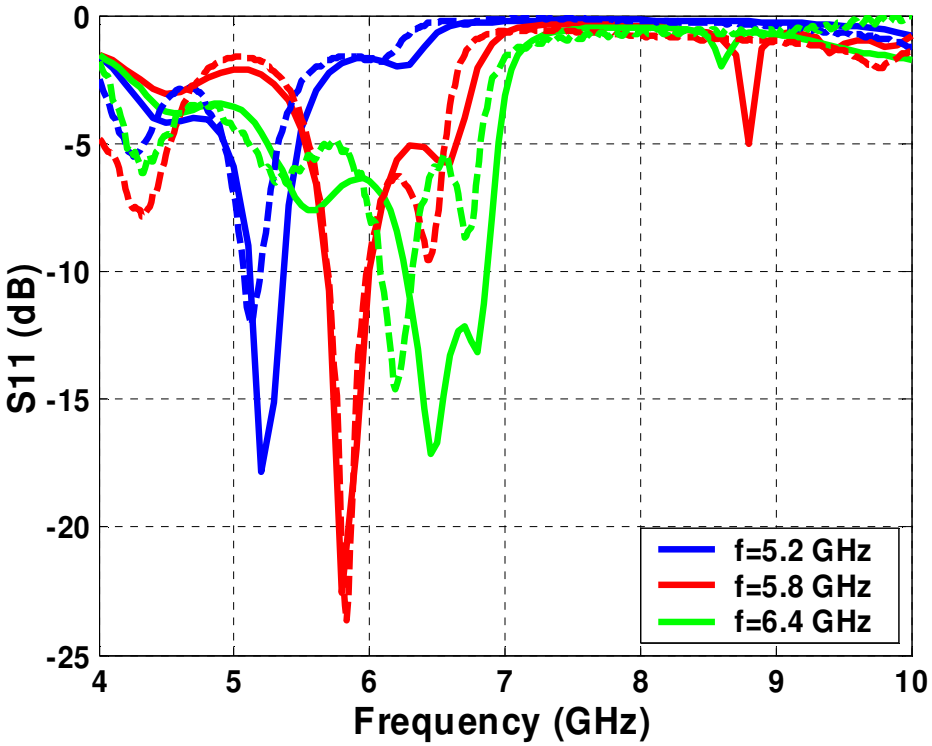

Figure 25. Simulation and measurement are presented for the three different frequencies. Simulation is presented in solid line and measurement is presented in dashed line

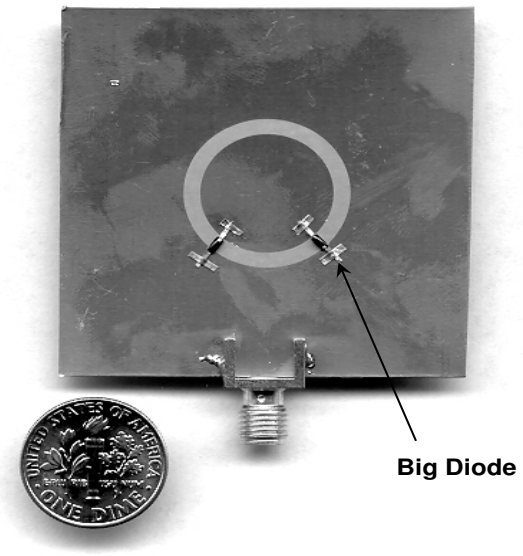

Figure 26. Photograph of the front side of the annular slot antenna. Two MBP-1035-E28 PIN diodes are observed, soldered symmetrically 45 from the feeding line.

The behavior of the diodes in both on and off state needs to be investigated. All the cases for which forward biased diodes are supposed to be used, are compared with hard-wire shorts. Therefore the suitable testing boards are fabricated and the performance of the diodes is evaluated through the agreement between the return loss measurements and the simulations. The comparison plots are presented in the following figures. For those cases where two diodes need to be forward biased simultaneously, two boards are fabricated and tested, substituting one diode at a time. The goal is to isolate the effect from each diode and finally evaluate the performance of the combined use of "small" and "big" diodes. The hard-wired boards are compared to the frequency reconfigurable design that operates in all the aforementioned frequencies. A layout of the back side of the antenna with the matching stubs designed as described in Section 3.2 is presented in Figure 27. For shorting and opening the stubs to the feeding line, ASI 8001 PIN diodes

are used, which will be referred to as 'small' diodes. Their length is less than 200 μm. On the annular slot, MBP-1035-E28 PIN diodes are used, which will be referred to as 'big' diodes. They are long enough to cover the 2 mm slot width. The matching network for the frequency reconfigurable design with a "big" diode biased at 45º along the ASA is shown in Figure 27. Three stubs of length L1, L3, and L2 are used to match the slot antenna to 5.2, 5.8, and at 6.4 GHz respectively. The dc bias lines are used to apply the dc voltage to the small diodes. When neither of the small diodes is biased, the antenna is matched at 5.8 GHz, by forward biasing the diode on the stub of length L1, the antenna is matched at 5.2 GHz, and by forward biasing the diode on the stub of length L2, the antenna is matched to 6.4 GHz. The reconfigurable matching network dimensions are presented in Table II.

In Figure 27 the 200 μm gaps (between the tapering small triangles and the feeding line) for the small diodes can be seen. The radial stubs are 70º wide and all the microstrip lines are 0.92 mm wide which results in a Zo of 50 Ω. The thin feeding lines are 120 μm wide and are used as dc bias lines. Their respective lengths are optimized for the frequency used, so they are equivalent to an open for the RF signal while they are perfect conductors for any applied dc current. The dc lines however are thin enough (very high RF impedance) to prevent leakage for the frequencies for which they are not optimized. Tapered segments are used to match the wider linear stubs to the small diodes in order to minimize reflections. The design procedure and the optimization of the matching stubs has been described in detail in section 3.2

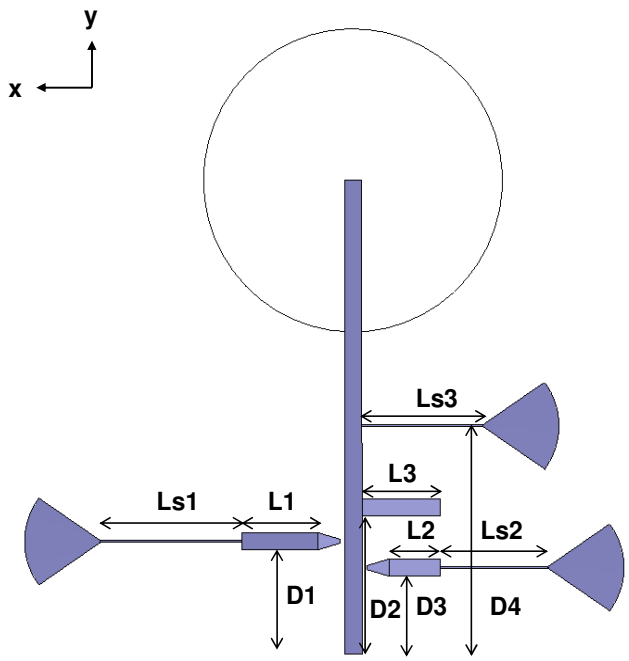

Figure 27 ASA frequency reconfigurable design matching network

TABLE II
Dimensions of circuit elements for frequency reconfiguration and null at 45°

Symbol	Value in mm
D1	5.49
D2	7.27
D3	4.10
D4	12.08
L1	4.05
L2	2.75
L3	4.21
Ls1	7.60
Ls2	5.75
Ls3	6.50

The antenna was fabricated on a 635 μm thick Rogers RO3006 substrate with ε_r=6.15 and tanδ=0.0025. The antenna is fed by a 50 Ω microstrip line. A standard photolithography technique was used for fabrication. The copper thickness was 18 μm and the alignment between the two copper layers was achieved by drilling holes on the substrate using a laser method. Big and small diodes can be seen in Figure 24 and Figure 26, respectively. A current smaller than 10 mA, was used to forward bias the diodes. For the small diode bias, dc bias lines were used and a wire carrying the bias was soldered to the radial stub. For the big diodes, the ground plane was grounded and a wire was soldered to the inner section of the ring. For return loss and radiation pattern measurements a 3.5 mm SMA connector was soldered at the beginning of the feeding line.

The small diodes are used to electrically connect the matching stubs to the transmission line. When the diodes are soldered onto the board but are not biased, they are equivalent to a small capacitive load. Their affect however is insignificant. That was verified in both return loss measurements and radiation pattern measurements. Return loss measurements to demonstrate the "small" diode effect are shown in Figure 28. When the diode is biased, the circuit is designed to match at 5.2 GHz, which is close to the measured resonant frequency in Figure 28. When the diode is not biased, the antenna is designed to be matched at 5.8 GHz. The measurement with the diode not biased is compared to the reference hardwired design of Figure 28 with no diodes on, and great agreement is observed.

For the simulation, the forward biased diodes were modeled as conductors. The small diode was modeled as a 0.2 mm x 0.25 mm 18μm thick Cu, and the big diode was

modeled as 2.2 mm x 1 mm perfect electric conductor. As a result the equivalent capacitance that

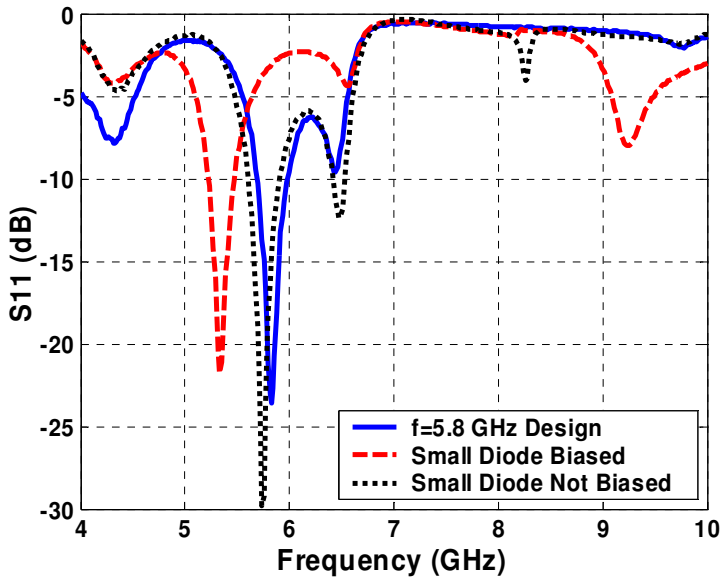

Figure 28. Small diode effect in the frequency reconfigurable design for the 5.2 GHz stub

appears when the diode is forward biased was not taken into consideration for the simulations and therefore a shift in the measured frequency appears compared to the simulation results.

The small diodes have different and less significant effect on the return loss compared to the effect of big diodes. The matching stub's length is optimized to cancel the imaginary part of the transmission line admittance at the resonance frequency. The existence of a small capacitance because of the diode package modifies the input imaginary part and consequently the length of the stub is no longer optimized for the design frequency. The combination of the capacitance and the stub is optimal for a "close" frequency and as a result, a small shift in the resonance frequency appears. The effect of the diodes in the return loss for the 5.2 GHz design and the 6.4 GHz design are

presented in Figure 29 and Figure 30 respectively. Generally the presence of a diode results in a shift of the resonance towards lower frequencies. Samples of the used fabricated boards are presented in Figures 31 and 32.

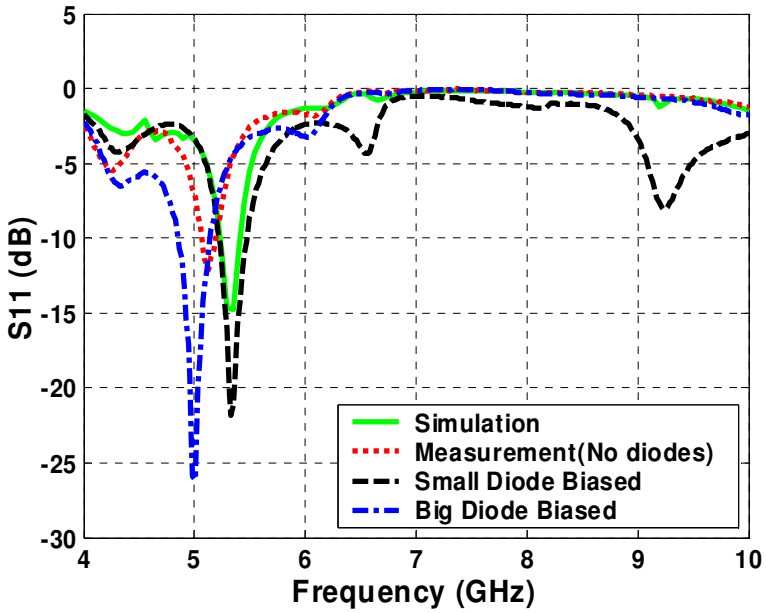

Figure 29. Diodes effect in return loss measurement for the 5.2 GHz design

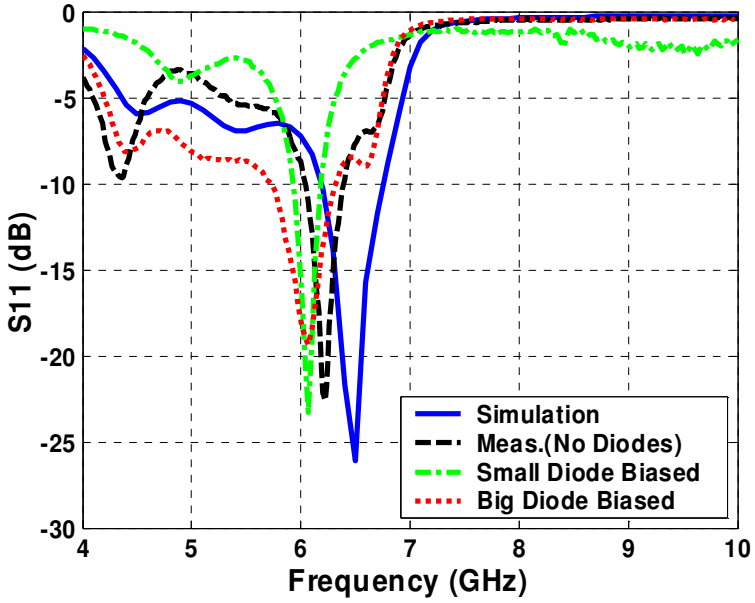

Figure 30. Diodes effect in return loss measurement for the 6.4 GHz design

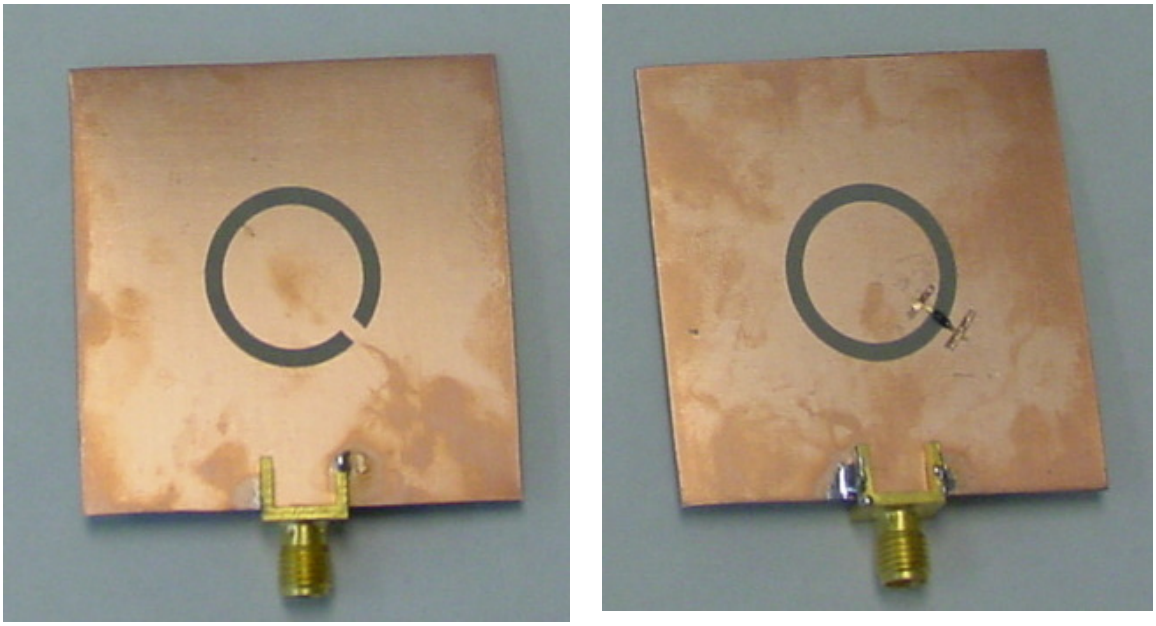

Figure 31. Fabricated samples The short on the slot is implemented with a hard-wired short or with a MBP-1035-E28 PIN diode

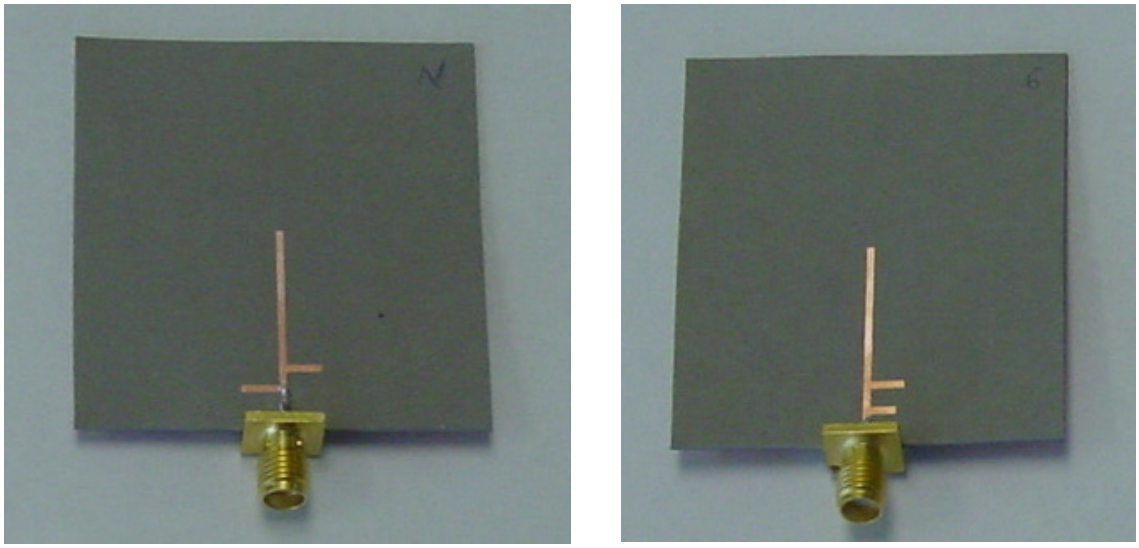

Figure 32. Fabricated matching stubs for 5.2 and 6.4 GHz

3.4 SUMMARY

In this chapter the proposed antenna structure with reconfigurable frequency has been analyzed. The slot presented is the shorted annular slot that has a null at 45^{o} direction with respect to the feed line direction. To match the antenna at three different frequencies linear matching stubs were used. PIN diodes were used for switches. The integration of the linear matching stubs with the diodes and the performance optimizations have been analytically described. The proposed design has been fabricated and tested, and return loss measurements results have shown very good agreement with the simulations. The effect of diodes on the return loss has been investigated and has proved to be minor. Therefore the effectiveness of the pin diode as a switch and the validity and accuracy of the simulated design have been verified. The behavior of the ASA and the effect of diodes for the pattern reconfigurable design will be presented and discussed in the next chapter.

CHAPTER 4

RADIATION PATTERN RECONFIGURABLE DESIGN

The pattern reconfigurability is a property highly desired for smart antennas. In this chapter the idea of rotating the null direction of the ASA radiation pattern is discussed. To change the direction of the null, pin diodes are used to create short circuits across the slot. Generally a null appears opposite to the position where the short is placed, but the short position must be tuned to compensate for discontinuity in the slot fields caused by the feed line to achieve the desired null direction with accuracy. The simulation results indicate that a null can be created anywhere between 15^{o} and 165^{o} by adding a short in the opposite direction. For a non-reconfigurable design, the short circuits may be hard-wired slotline short circuits, but in the reconfigurable design, they are implemented with pin diodes. The short in the slot results in a reformation of the electric field distribution along the slot leading to a shift of the null in the short direction. It also changes the equivalent load at the input of the microstrip transmission line; therefore, reconfigurable matching stubs are required to keep the antenna matched at the design frequency during null reconfiguration. To explain the null position, and the shift in null position that is observed when the mean slot circumference is perturbed from the $3\lambda_s/2$ length, a simple but accurate theoretical model is proposed. The analytical expressions deduced by the three magnetic dipoles that consist the model, are verified by the numerical solution and the measurements. The proposed design is fabricated and tested. In order to demonstrate the pattern reconfigurability the central frequency f=5.8 GHz is selected. The resonance frequency is maintained constant while the null shifts in three positions. Return loss measurements and radiation pattern measurements are presented that verify the model validity and demonstrate the design's agility.

4.1 THEORETICAL ANALYSIS

4.1.1 PATTERN RECONFIGURABLE PRINCIPLES

The radiation patterns of the shorted ASA yield a null in a direction different than the feeding line direction, which is the case for the regular, unperturbed slot. The E field distribution along the slot for the unperturbed slot is presented in Figure 33 while the E field distribution for the shorted slot is presented in Figure 34. It is obvious from the field distribution plot that the field pattern and consequently the far field radiation pattern is rotated by 45^{o}. The simulated 3-D radiation patterns are presented in Figure 35 and Figure 36 for the unperturbed and shorted ASA respectively. All the simulations presented so far involve the 5.8 GHz frequency. The simulated x-y plane radiation patterns for the case of a hard-wired short circuit at 225º are presented in Figure 37. In Figure 37 and all subsequent figures x-y axes are used. The x axis corresponds to φ=0º and the y axis to the φ=90º. The radiation patterns and all references on angle positions are consistent with the aforementioned notation. In that plane the E field is polarized in φ direction, parallel to the slot plane. The null is created in the x-y plane instead of the broadside direction because it is meant to decrease the effect of an interferer coming from a direction different than the directivity (maximum field value) direction, which is parallel to z axis. At 5.8 GHz, for which the slot dimensions are optimized, a null exists exactly opposite to the slot short with respect to the slot center. At 6.4 GHz, the null appears approximately 10º closer to the 90^{o} direction, while at 5.2 GHz, the null deviates from the 90^{o} direction and moves closer to the 0^{o} direction by 5º. Similarly, placing a short circuit at 315º, results in a null in the radiation pattern at 135º for 5.8 GHz. As a more general concept, when a frequency lower than the design frequency is used, the null

shifts towards the φ=90° direction while it shifts towards the φ=0° direction when a higher frequency than the design frequency is used.

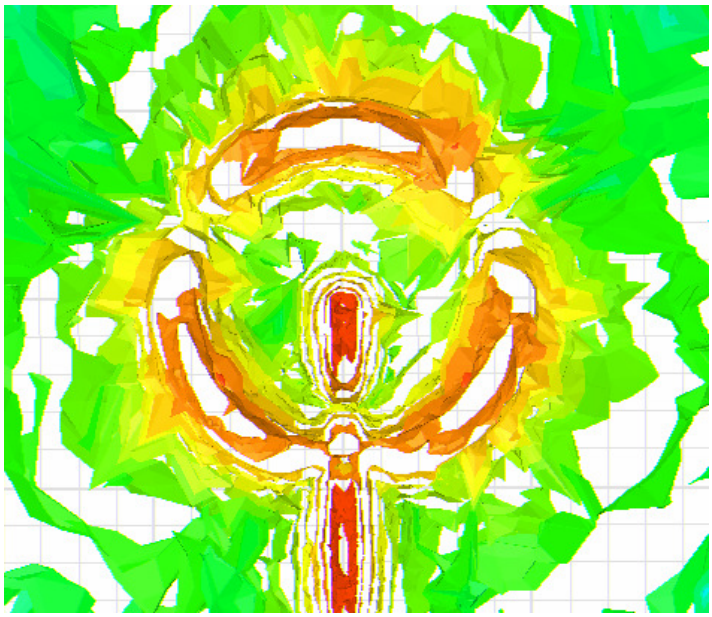

Figure 33. E field distribution for unperturbed (no shorts) annular slot antenna

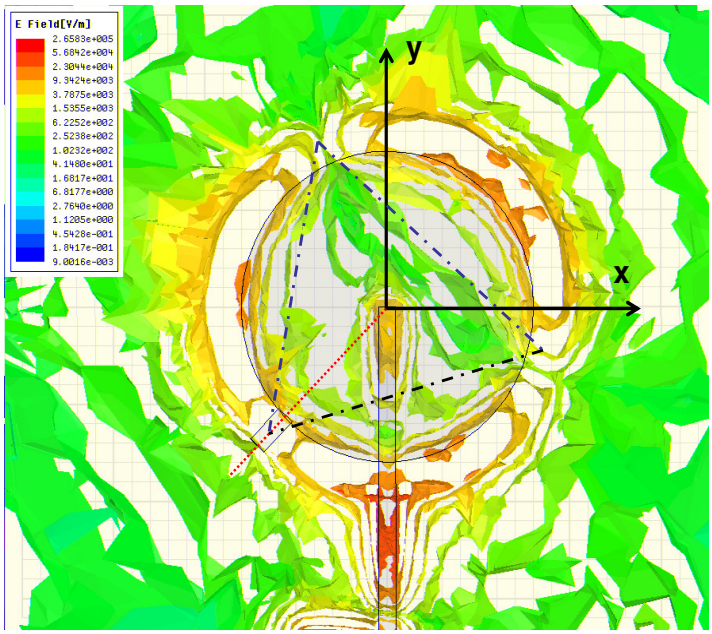

Figure 34. Electric field distribution for f=5.8 GHz when a short is placed at 225°. The dipoles model is superimposed for comparison

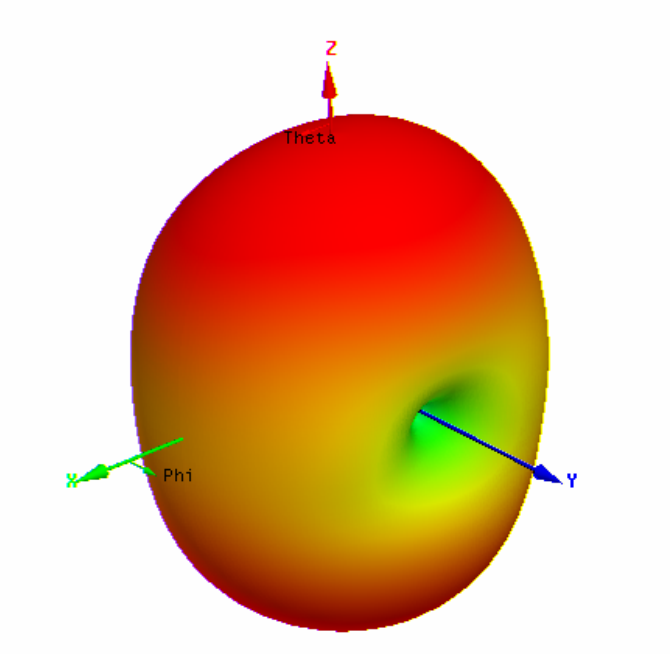

Figure 35. 3-D radiation pattern that presents a null in the feed line direction (y axis) for f=5.8 GHz

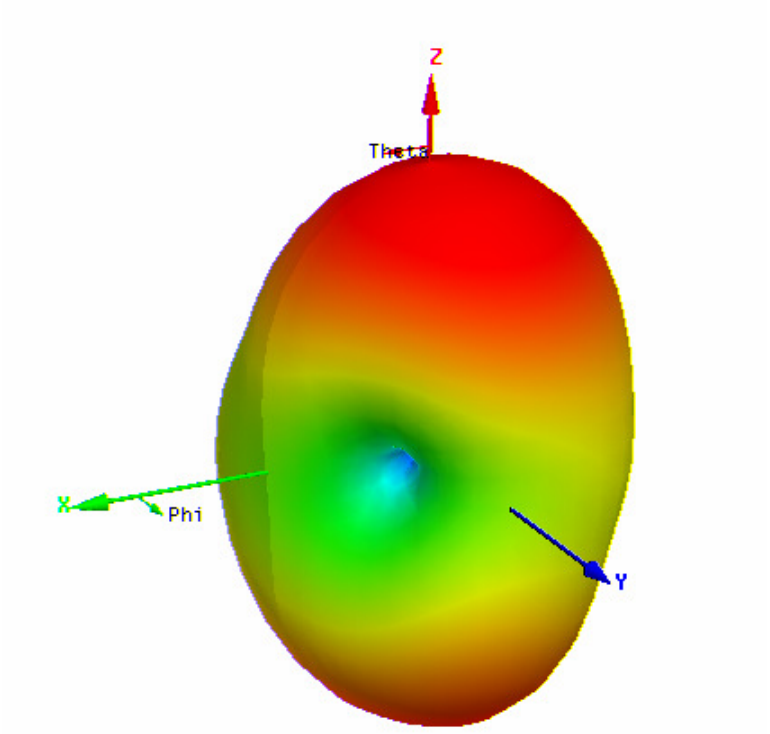

Figure 36. 3-D radiation pattern that presents a null in the 45^{o} direction when a short is used at 225 ^{o} along the slot circumference for f=5.8 GHz

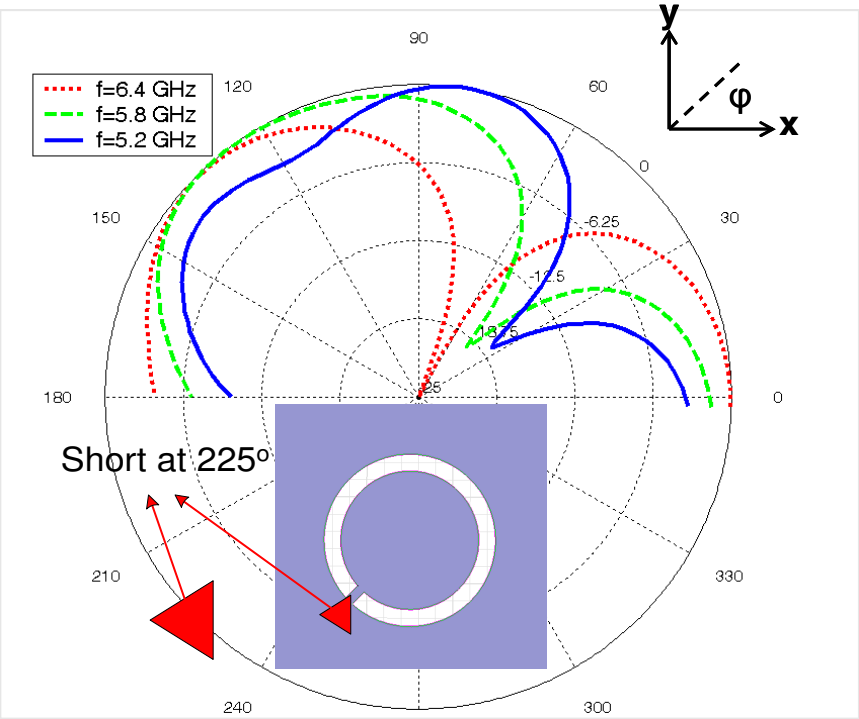

Figure 37. Simulated normalized radiation patterns on the x-y plane with a short circuit at 225º. The null direction for the slot without any short would be in the 90º direction with respect to the plot labeling.

As discussed, varying the null position changes the impedance of the antenna and requires a reconfigurable matching circuit. When a short is placed at 45º from the feeding line, as shown in Figure 37, a single stub with length 4.21 mm and width 0.92 mm at a distance of 7.27 mm from the feeding point is used to match this short position at 5.8 GHz. The exact layout for the null reconfigurable design will be discussed in detail in the next section. When the short is removed, simulating the case that the diode is not biased, a second stub must be added as a shunt matching device at the feeding line in order that the resonance frequency remains constant. The technique to define the stubs' length and their position is explained in chapter 3. Return loss simulation and measurements are presented in Figure 38, where it is seen that a 5.8 GHz resonant frequency is maintained

regardless whether or not a short exists. The 4.5 GHz parasitic resonance, when no short circuits occur on the ring, is easily removed by filtering it with a microstrip passband filter that can be cascaded to the antenna geometry.

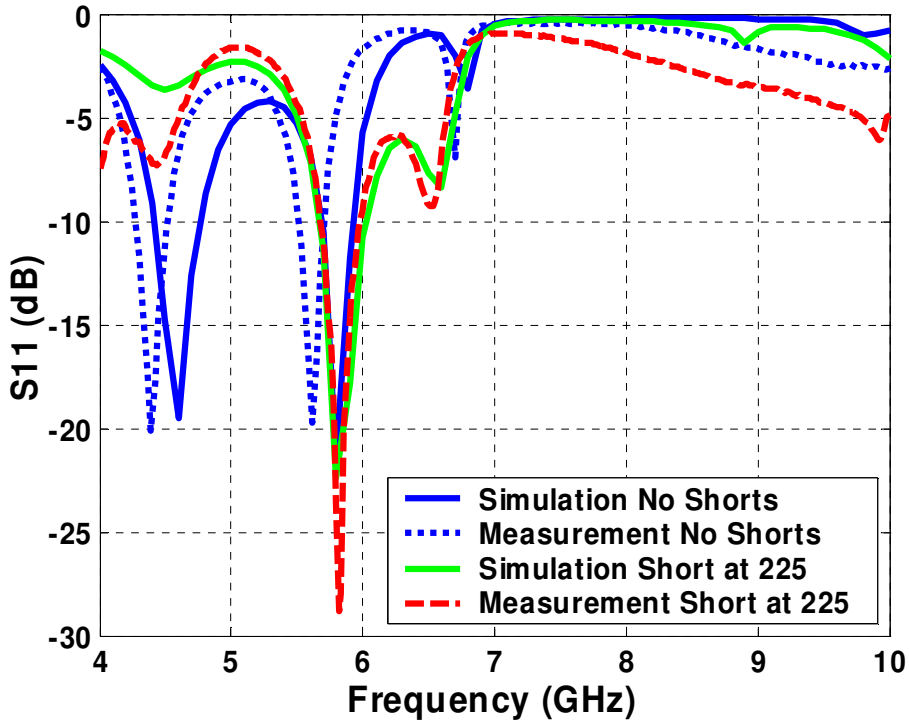

Figure 38. Simulation and measurement results for the null reconfigurable design The first two lines refer to the design without any short. The numbers in the label refer to the hard-wired short position compared to the polar plot label in Figure 37.

4.1.2 THREE DIPOLES MODEL

To qualitatively explain the shift in the null direction when a short is placed along the slot, a novel but simple model using magnetic dipoles is introduced and briefly discussed. The field distribution as a result of a numerical simulation using HFSS [29] was presented in Figure 34. Based on the field distribution, the dipole model presented in Figure 39 is proposed, which consists of three magnetic dipoles of length $\lambda_s/2$ with sinusoidal magnetic current excitation. The $\lambda_s/2$ magnetic dipole is the dual equivalent to

the λ/2 electric dipole. The electric field component E on a plane that includes an electric dipole with length 'l' is given by [30]. Based on the duality principle [30] the E field derived from a magnetic dipole is presented in (1), where k is the wavenumber, r is the distance from the dipole's center and M_o the amplitude of the magnetic current excitation. The angle θ is the elevation angle measured from the z axis which is parallel to the dipole. The dipoles for the proposed model lay on x-y plane therefore the azimuthal angle φ is used in (2) but the expression applied for each one dipole is still the expression in (1).

$$E(\theta) \simeq -j\frac{M_o e^{-jkr}}{2\pi r}\frac{\cos\left(\frac{kl}{2}\cos\theta\right)-\cos\left(\frac{kl}{2}\right)}{\sin\theta} \qquad (1)$$

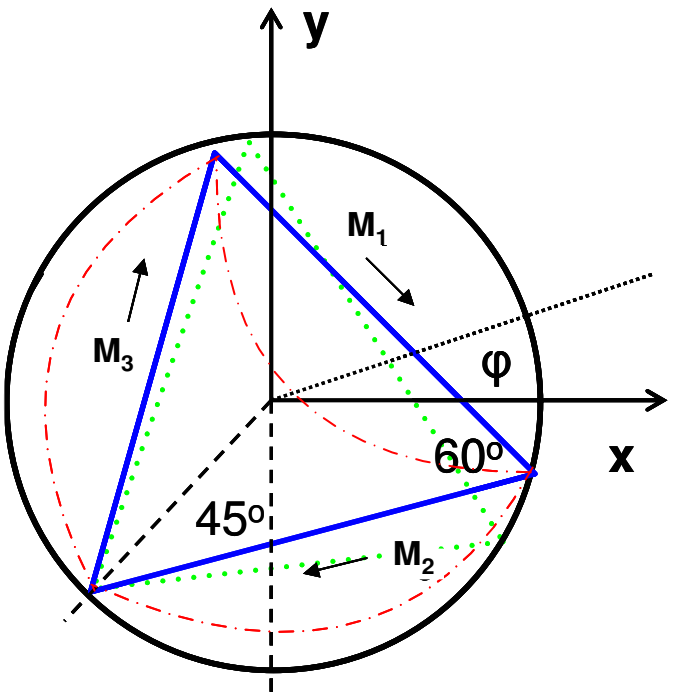

Figure 39. Magnetic dipoles model of ASA with short circuit at 225º. Three dipoles are used in equilateral triangle orientation (Blue solid lines are for 5.8 GHz and green dotted lines for 5.2 GHz).

The superimposed electric field as a result of all three dipoles is given by (2) and is plotted in Figure 40 in polar coordinates.

$$E = \left| e^{j\delta_1} E_1(\phi + \frac{\pi}{4}) + e^{j\delta_2} e^{-jkd_2} E_2(\phi + \frac{\pi}{4} + \frac{2\pi}{3}) \right. \\ \left. + e^{-j\delta_3} e^{-jkd_3} E_3(\phi + \frac{\pi}{4} - \frac{2\pi}{3}) \right| \quad (2)$$

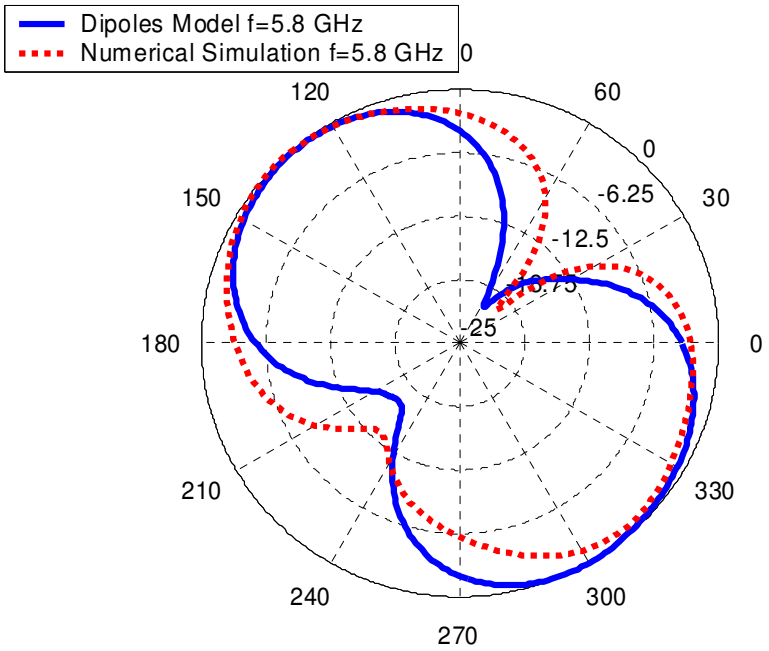

Figure 40. Analytical expression plot of ASA with short circuit at 225º compared to the numerical solution for the amplitude of **E** field.

The phase shift π/4 is used to take into consideration the respective dipoles' orientation with respect to the reference axes. There is also a 2π/3 angle between two consecutive dipoles which must be considered. In Figure 41 and Figure 42 the magnetic current and phase distribution along the annular slot, are presented as derived from the

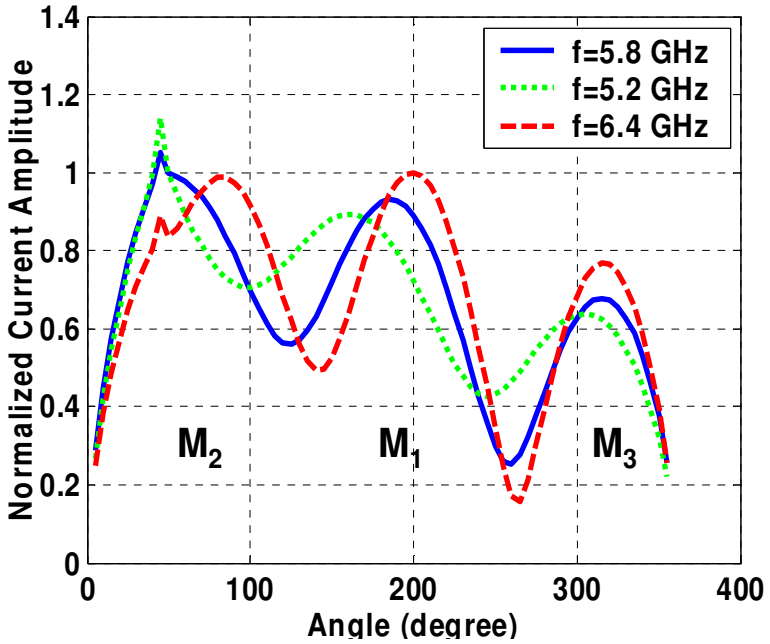

Figure 41. Magnetic Current amplitude distribution along the annular slot

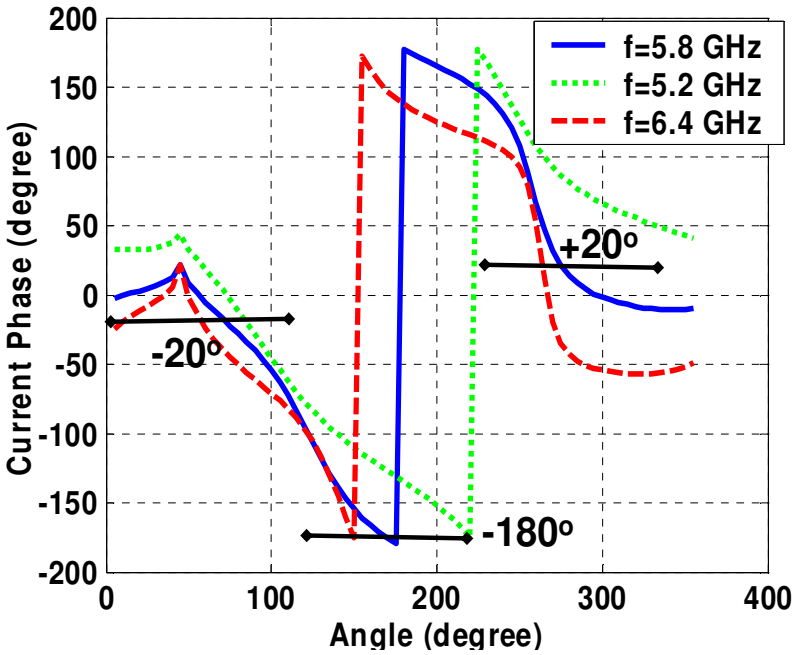

Figure 42. Magnetic current phase distribution along the annular slot The 0 corresponds to the short position. The singularity at 45° is due the excitation source. The phases and normalized amplitudes correspond to M_2, M_1 and M_3 from left to the right.

electric field distribution presented in Figure 34. The magnetic current distribution presented in Figure 41 matches the magnetic current distribution calculated and measured for the shorted annular slot, presented in [5].

For expression (2) the amplitude and phase for each magnetic current excitation must be estimated. The phases and amplitudes for the dipoles' currents for f=5.8 GHz are calculated from the solid lines in Figure 38 using the technique applied in [31]. The phases, δ_1, δ_2 and δ_3 are the phases of the current excitations and are calculated as the mean values of the continuous phase distribution in the corresponding segment, as shown in Figure 42. Therefore from Figure 42 the phases are estimated as $\delta_2=-20^o$, $\delta_1=-180^o$ and $\delta_3=20^o$. The current amplitudes are normalized with respect to the strongest current M_2, which is the current on the segment where the excitation is applied. From Figure 41 $M_1=0.9M_2$ and $M_3=0.7M_1$ are deduced. The amplitudes descent in that order, because of the traveling wave which is excited on the ring that attenuates as it propagates away from from the excitation source. The path difference between E_1 and E_2, is $d_2=(\lambda/4)\cos(60-\varphi)$ while the path difference between E_1 and E_3 is $d_3=(\lambda/4)\cos(60+\varphi)$ and can be easily deduced geometrically from Figure 43. d2=(AA1). From orthogonal triangle AA1B AA1= (AB)*cos(60-φ) where (AB)=λ/4. Similarly d1=(BB1) and from orthogonal triangle CB1B (BB1)=(BC)*cos(60+φ) The normalized magnetic current excitations and the phases used, apply for any design frequency for which the annular slot length is $3\lambda_s/2$. The antenna prototype can be scaled for a different frequency without affecting the validity of the model.

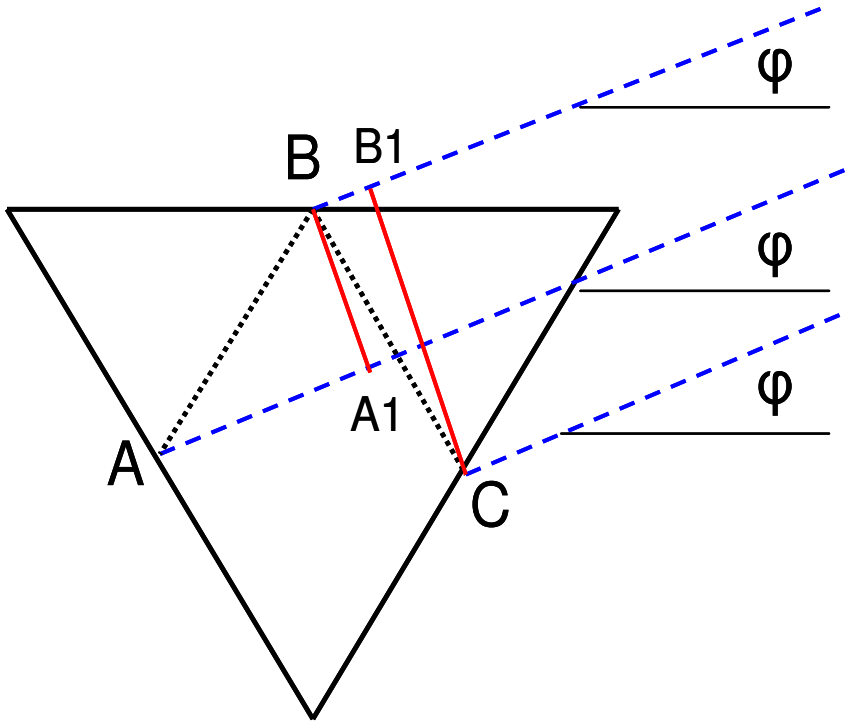

Figure 43. Three dipoles in equilateral triangle orientation

The analytical model predicts the null position and matches the numerical solution with satisfactory precision as shown in Figure 40 for the central frequency, f=5.8 GHz. Measurements and the numerical solution show a shift in the null position as the frequency changes, which is predicted by the dipole model. At a different frequency, the slot circumference is no longer $3\lambda_s/2$ and a different field distribution occurs. As a result the magnetic dipoles do not maintain their orientation with respect to the axes, but they rotate slightly instead. For the lower frequency, the wavelength is about 10 % longer and therefore the magnetic dipoles structure is rotated clockwise with the point at the short fixed. The current distribution for f=5.2 GHz, for the dipole with M_2 excitation requires a longer segment along the ring (dotted line Figure 41) compared to the current 5.8 GHz. The $\lambda_s/2$ length at 5.2 GHz is about 10% longer than the one for 5.8 GHz so the dipoles

structure is rotated clockwise with the point at the short fixed (dotted straight lines in Figure 39). The dipole with currents M_1 and M_3 behave accordingly. The dipole with M_2 needs to be slightly shorter than $\lambda_s/2$ since it terminates at the short position and it overlaps with the feeding line. However it still remains close to $\lambda_s/2$. Therefore the same analytical expression (2) is used with the offset angle to be slightly greater than $\pi/4$. That results in the rotation of the entire radiation pattern by the same offset angle clockwise as can be seen in Figure 40. For the same reason, the use of a higher frequency at 6.4 GHz results a counter-clockwise rotation of the null direction. The proposed model aims primarily to give a qualitative explanation in the null shifting; therefore absolute agreement with the numerical solution should not be expected. The microstrip feed line and the matching circuits, which are only on one side of the ASA only, destroys the symmetry. Therefore the null is stronger in the direction opposite to the feeding line as can be seen in Figure 40 where the simulation results in all 4 quadrants are presented.

4.2 NULL POSITION RECONFIGURABLE DESIGN

For the null reconfigurable design, two stubs are used to match the antenna for the two cases; when there is a short at ±45º away from the feeding line, and when no short exists along the circumference. Consequently one small diode is used for the activation of the matching stubs and two big diodes for the null control. When the small diode is not biased and one of the two big diodes is biased, the antenna is matched at 5.8 GHz and gives a null at 45^o. When none of the big diodes are biased and the small diode is biased, the antenna is matched at 5.8 GHz and a null appears in the direction opposite to the feeding line. This second stub is placed at a distance D1=4.75 mm and has length L1=2.97 mm. As a result, for a fixed frequency at 5.8 GHz a null in three different

directions (-45º, 0º, and +45º) can be created. The matching network design is presented in Figure 44 and the dimensions are presented in Table III. The return loss measurements for the hard-wired samples in comparison with the simulated results were presented in Figure 38. The measurements for the samples with the diodes are presented in Figure 45.

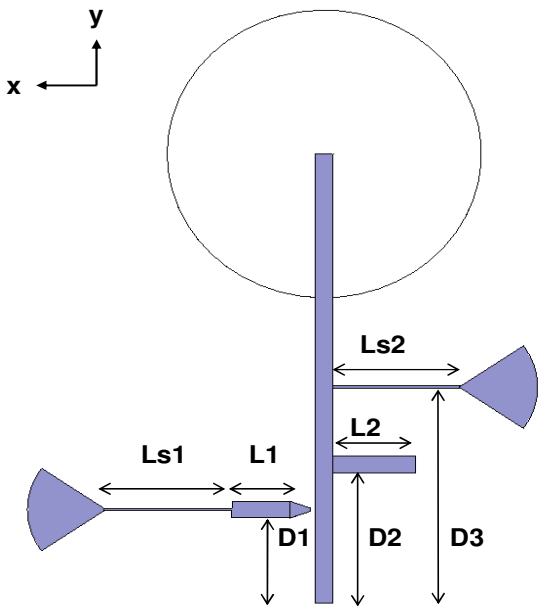

Figure 44. ASA Null reconfigurable design matching network

TABLE III
Dimensions of circuit elements for null reconfiguration at 5.8 GHz

Symbol	Value in mm
D1	4.75
D2	7.27
D3	12.08
L1	2.97
L2	4.21
Ls1	6.50
Ls2	6.50

A small shift in the resonance frequency is consistently observed when a big diode is biased along the slot. The capacitive load on the circumference results in a downwards shift of the resonance frequency as discussed in [13]. For the null reconfigurable design, the coexistence of two diodes on the slot with one of them forward biased and the second one reverse biased results in a parasitic resonance close to 6.5 GHz, as seen in Figure 45. This is because of the additional capacitive load as a result of the reverse biased diode. The parasitic resonance can be filtered with a cascaded microstrip passband filter for the single frequency (5.8 GHz) null reconfigurable antenna. For the extension to multiple frequencies, the parasitic will be taken care of with the appropriate matching configuration. For the simulation, the reverse biased diode was simulated as a perfect open and that is why the parasitic resonance does not appear in the simulation. There is still a good resonance at the design frequency which is consistent for all three directions of the null and is measured at 5.65 GHz which is less than 3% off the design frequency.

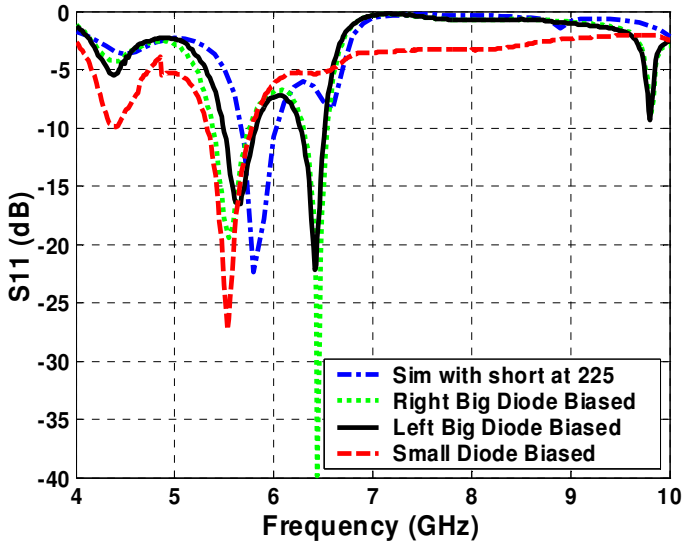

Figure. 45. Diodes effect in return loss measurement for the null reconfigurable design. The design frequency was 5.8 GHz.

4.3 RADIATION PATTERN MEASUREMENTS

A far field antenna test range was used to characterize the ASA. In the test range, the ASA was the receiving antenna that rotated through the ϕ plane while a 5.4-8.2 GHz, 15 dB standard gain horn was used as the fixed, transmitting antenna; the two antennas were separated by 1 m. The transmitted RF signal was AM modulated by a 20 MHz signal that was detected by a diode detector and measured by a lock-in amplifier. Control of the rotary stage, lock-in amplifier, and data recording was automated. To bias the diodes, wires were soldered to the center of the ASA and the radial stubs of the matching circuit. In addition, a bias tee was used to ground the microstrip line and to isolate the applied bias from the diode detector. Because the ASA radiates backward as well as forward, the coaxial launcher, bias tee, and detector were sandwiched between 1 cm thick pieces of absorbing material. Before characterizing the ASA, a variable attenuator was used to vary the input power in order to calibrate the diode detector and determine the radiated power that results in maximum detector sensitivity. During test, it was observed that the substrate corners had to be rounded (Figure 46) to minimize reflections and diffractions at the corners that caused ripples in the radiation pattern. A measurement taken before the corners were rounded is presented in Figure 47. The ripple in the 135^{o} direction because of the diffraction on the board corner is obvious.

The effect of both the small and big diodes on the radiation patterns was investigated and is presented in the current section, and the radiation patterns are compared to the simulation results (ideal elements) and to the hard-wired design measurements presented earlier. In Figure 48, the measured radiation patterns for the E_{φ}

component of the electric field, which is the component parallel to the antenna substrate, for all three frequencies and

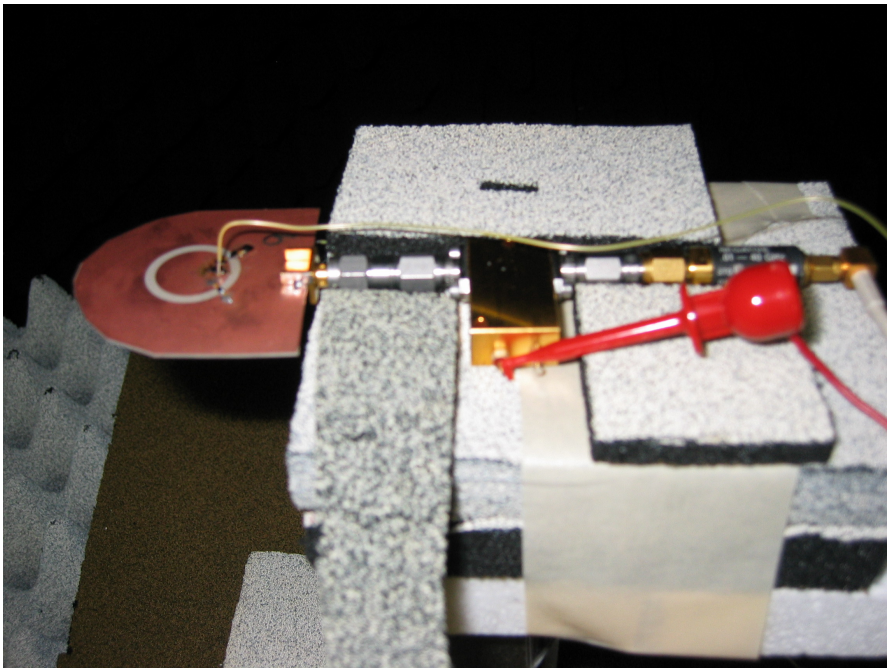

Figure 46. Photograph of the tested ASA with the rounded corners. The dc probes for the diodes bias can be seen.

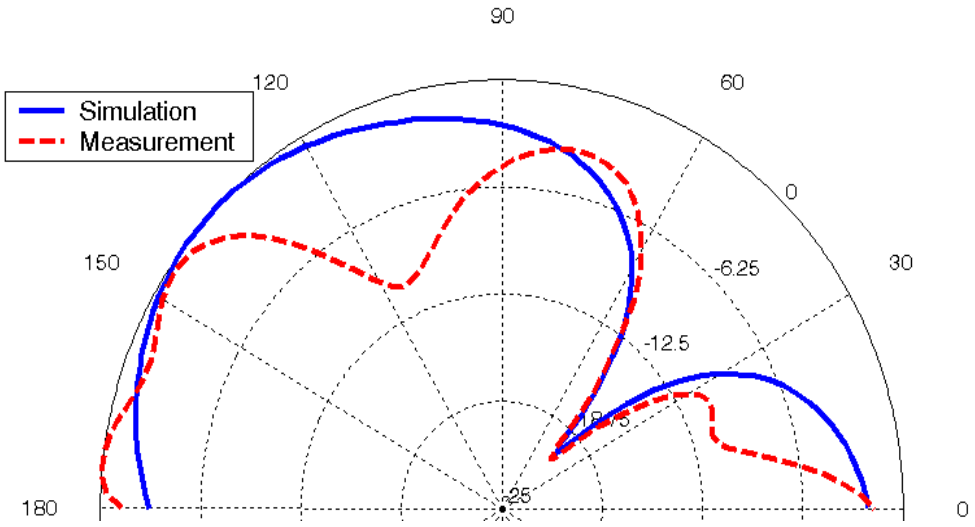

Figure 47. Eφ radiation pattern at 5.8 GHz with the short along the slot circumference

a hard-wired short at 225º are shown. In addition, the measured radiation pattern at 5.2 GHz for a regular slot without any short along the slot is shown. The results in Fig. 44 have similar behavior to the simulated results presented in Figure 37 in section 3.1. The shift in the null direction with respect to the frequency that was explained in a previous section is hereby verified experimentally.

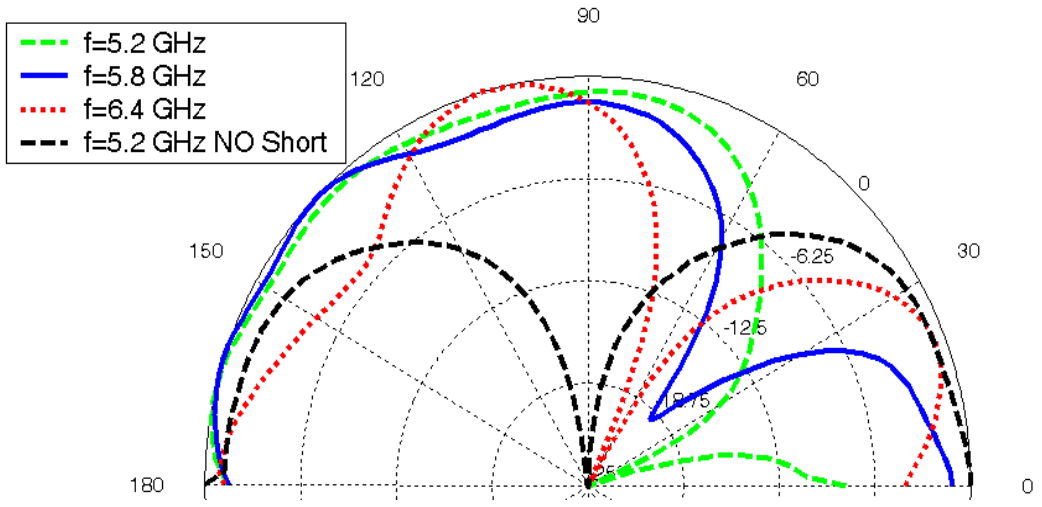

Figure 48. Measured radiation patterns for the design frequencies when a hard- wired short is placed at 225^{o}

Figure 49 and Figure 50 present the measured radiation patterns for frequencies of 5.2 GHz and 6.4 GHz respectively with diodes used to short the slot. They were in very good agreement with the simulation and the hard-wired measurements. This proves that the PIN diode is a suitable switch for this application. The effectiveness of the small diodes has been verified in designs other than antennas, like filters [32] and it only has to do with the matching network. The parasitic capacitance and resistive load of the big diodes that differentiate them from the ideal short circuit, on the other hand, have been

hereby proven experimentally not to distort the radiation pattern in comparison to the ideal elements.

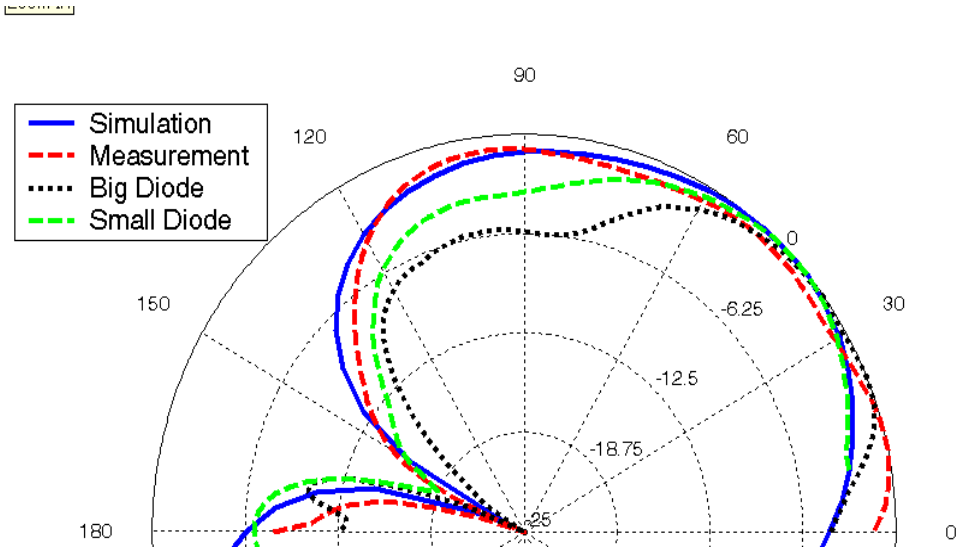

Figure 49. Radiation patterns for the 5.2 GHz frequency design when the short is placed at 315°. Simulation, measurement with hard-wired short, measurement with the big diode biased, and measurement with the small diode biased are presented

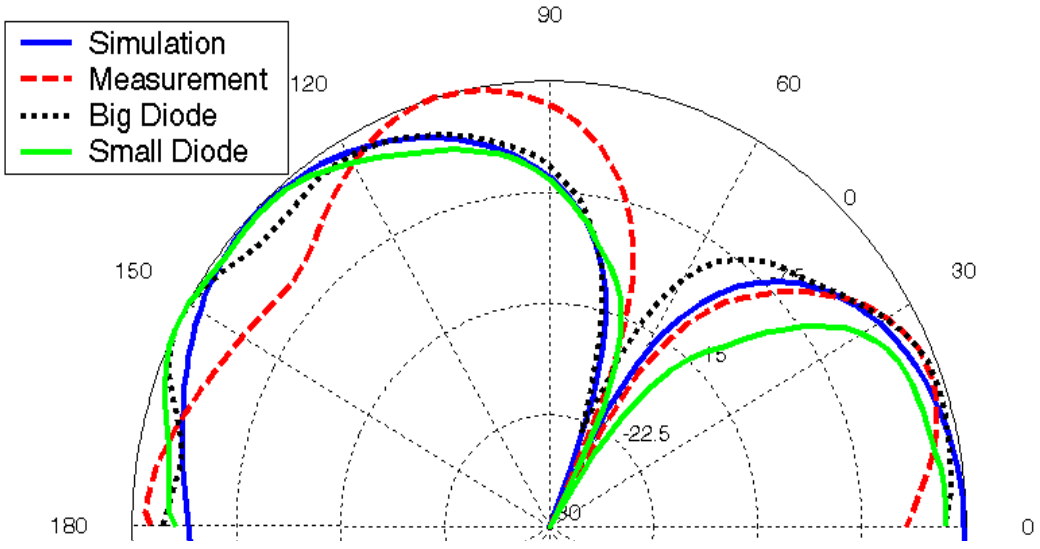

Figure 50. Radiation patterns for the 6.4 GHz frequency design when the short is placed at 225°. Simulation, measurement with hard-wired short, measurement with the big diode biased, and measurement with the small diode biased are presented.

The short was placed in symmetrical positions with respect to the feeding line direction in order to show that the results are not dependent on the side of the short and are not affected from the non symmetric matching stubs. The behavior of the antenna is equivalent for both sides of the short.

In the plots presented in Figures 49 and 50, the measurements were taken for different samples in order to compare and evaluate the effect of small and big diodes independently. For the null reconfigurable design (Figures 51 and 52) all measurements were taken for the same sample on which three diodes are used and biased individually to steer the null in the three directions and maintain a constant resonant frequency. In order to get the nulls in the side directions, the corresponding big diode is biased. In order to get the null in the feeding line direction, the small diode on the matching stub L1 in Figure 44 is biased in order to maintain the resonance frequency constant at 5.65 GHz while none of the big diodes is biased. In Figure 51 and Figure 52 where the simulated and measured results are presented, respectively, it is obvious that the steering of the null is achieved with high precision. The slot dimensions are optimized for the frequency of 5.8 GHz and for that frequency the null is exactly at 45^{o} off the feed line direction. The measured patterns are for f=5.65 GHz which is very close to the design frequency and as a result the null directions verify the simulation with high accuracy. In the 90^{o} direction the simulated field is stronger than the measurement but overall good agreement is demonstrated.

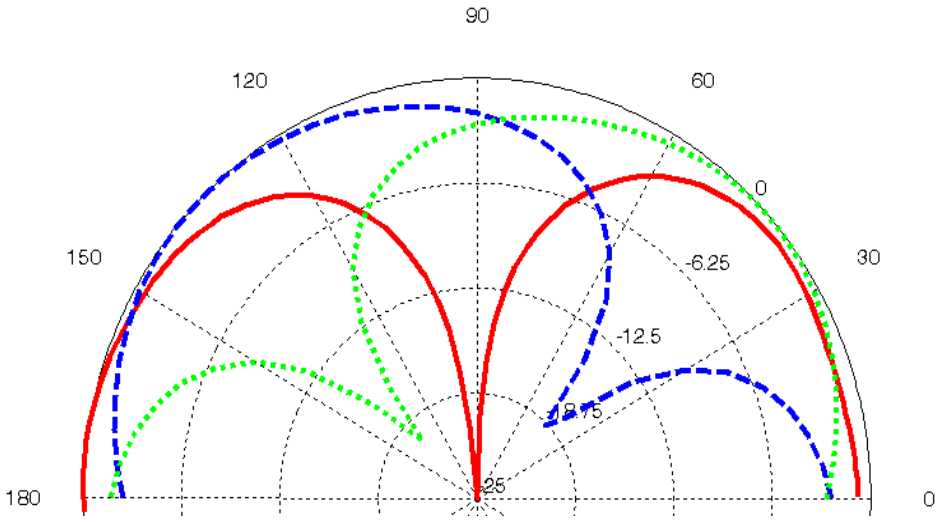

Figure 51. Simulated radiation patterns in x-y plane for the null reconfigurable design at f=5.8 GHz. The null is directed at 45°, 90°, and 135° direction. The 90° direction is the null direction when no short is used

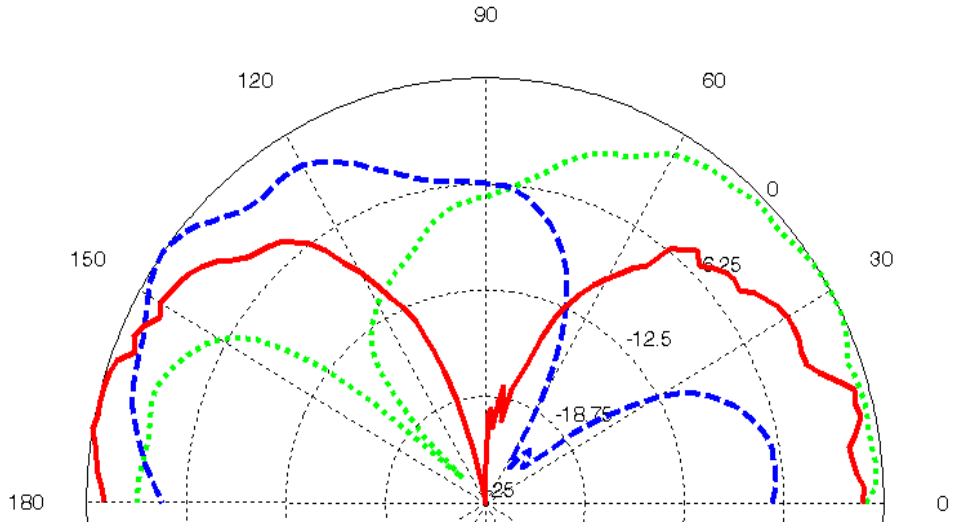

Figure 52. Measured radiation patterns in x-y plane for the null reconfigurable design at f=5.65 GHz. The null is directed at 45°, 90°, and 135° direction using two PIN diodes placed at. 225° and 315° .The 90 ° direction is achieved when none of the diodes is biased.

4.4 SUMMARY

The null position reconfigurable design has been presented in this chapter. The null position has been steered using switches implemented with pin diodes along the aperture circumference. This behavior has been analyzed in detail with a novel, simple but accurate model using three magnetic dipoles in equilateral triangle orientation to substitute the magnetic current within the slot. The model has justified adequately the reorientation of the null when a short is used to load the slot, and the small shift in the mull position when the slot circumference is perturbed from the optimized $3\lambda_s/2$ length.

The proposed antenna was fabricated and tested. The use of diodes and their performance compared to hard-wire shorts has been demonstrated. The radiation pattern measurements were in good agreement with the simulated results. The measurements procedure has been described and experimental techniques have been suggested to overcome measurements inconsistency.

The radiation pattern analysis and the experimental verification conclude the study on the proposed reconfigurable in frequency and radiation pattern Annular Slot Antenna.

CHAPTER 5

CONCLUSION AND POTENTIAL APPLICATIONS

The goal of this thesis has been to develop and optimize a single antenna that would demonstrate a reconfigurable frequency of operation and a reconfigurable radiation pattern. This antenna has been designed to operate in a very popular frequency range where a great number of wireless communication applications exist. From this analysis, it has been concluded that a successful, low cost reconfigurable antenna design has been introduced to the wireless and radio frequency design community.

A new design for both pattern and frequency reconfigurable annular slot antenna was presented. Matching stubs were used to match the antenna to three different frequencies, 5.2 GHz and 6.4 GHz in addition to the initial central frequency at 5.8 GHz. PIN diodes were used to connect or disconnect the stubs creating a reconfigurable matching network. The radiation pattern control was achieved by activating/deactivating shorts on the slot. As a result the null was redirected to a different direction. As a benchmarking approach, the shorts were implemented by use of pin diodes. When each diode was forward biased, it was equivalent to a short, and when it was reverse biased, it behaved as a capacitive load. In the latter case, when no diodes were forward biased, the slot antenna behaved like the unloaded slot antenna and the null appears in the feeding line direction. The results for this antenna were presented at three separate frequencies.

Any other frequency can be matched using the same technique as long as the radiation efficiency for that frequency is satisfactory. The same applies with the position of the shorts. The possible directions are not limited to the ones used in this study but in

that case also, the matching stubs need to be redesigned and optimized for the preferred short direction, since the short direction affects the equivalent load at the end of the transmission line. The measured results were compared to the simulations and were found to be in very good agreement. The proposed antenna is compact and easy to integrate with other microwave components.

There is a great number of applications for this kind of reconfigurable antenna. This antenna is the first step towards more mature compact reconfigurable slot antennas both in frequency and radiation pattern using pin diodes or RF MEMS switches. The ASA can be used as a mobile device antenna, although the fact that direction of the interferer is completely random would require a more sophisticated and complicated antenna structure. The antenna can find application in cases where interference in the x-y plane needs to be minimized. In practical scenarios, this can be useful if combined with a mechanical motion of the antenna where the plane of the antenna can also be moved. Another application could be the interference minimization in an antenna array environment. The proposed antenna can be used as planar array element. In a reconfigurable array, where different combination of elements can be active at a time, the creation of nulls in pre-selected desired positions give a design parameter to control the mutual coupling between neighboring elements. At the same time, the directivity in the broadside direction remains equally high.

APPENDIX A

LIST OF PUBLICATIONS

[1] **S.Nikolaou**, G.E.Ponchak, J.Papapolymerou and M.M.Tentzeris, "Shorted Annular Slot Antenna (ASA) Matched at Three Different Frequencies", IEEE-APS Symposium, Washington, DC, July 2005

[2] **S.Nikolaou**, G.E.Ponchak, J.Papapolymerou and M.M.Tentzeris, "Design and Development of an Annular Slot Antenna (ASA) with a Reconfigurable Radiation Pattern" Accepted for presentation in APMC 2005 Asia-Pacific Microwave Conference Suzhou, China, December 2005**.**

[3] **S. Nikolaou**, R.Bairavasubramanian, C. Lugo Jr.,I. Carrasquillo, D.C. Thompson, G.E. Ponchak, J. Papapolymerou, M. M. Tentzeris, "Pattern and Frequency Reconfigurable Annular Slot Antenna using PIN Diodes." Accepted for publication in IEEE Transactions on Antennas and Propagation, February, 2006

REFERENCES

[1] D. M. Pozar, "Reciprocity method of analysis for printed slot and slot–coupled microstrip antennas", IEEE Transactions on Antennas and Propagation, Vol. AP-34, pp. 1439 – 1446, 1986

[2] A. Axelrod, M. Kilsiuk, and J. Maoz, "Broadband microstrip-fed slot radiator", Microwave J., pp.81-94, 1989.

[3] Garg, P. Bhartia, I. Bahl, A. Ittipibbon, " Micostrip antenna design handbook", Artech House, pp. 441-491, 2001

[4] H. Morishita, K. Hirasawa, and K. Fujimoto, " Analysis of a cavity-backed annular slot antenna with one point shorted", IEEE Transactions on Antennas and Propagation, vol. 39, no.10, pp. 1472 – 1478, October 1991.

[5] J.T. Bernhard,R. Wang, R. Clark, and P. Mayes, "Stacked reconfigurable antenna elements for space-based radar applications", IEEE Antennas and Propagation Society International Symposium, Vol. 1, pp. 158 – 161, July 2001.

[6] K. Tomiyasu, "Conceptual reconfigurable antenna for 35 GHz high-resolution spaceborne synthetic aperture radar", IEEE Transactions on Aerospace and Electronic Systems, Vol. 39, Issue: 3, pp. 1069 – 1074, July 2003.

[7] J.T. Aberle, Sung-Hoon Oh, D.T. Auckland, and S.D. Rogers, "Reconfigurable antennas for wireless devices" IEEE Antennas and Propagation Magazine, Vol. 45, Issue: 6 , pp. 148 – 154, December 2003.

[8] G.H. Huff, J. Feng, Shenghui Zhang, G. Cung, and J.T. Bernhard "Directional reconfigurable antennas on laptop computers: Simulation, measurement and evaluation of candidate integration positions", IEEE Transactions on Antennas and Propagation, Vol. 52, Issue:12, pp. 3220 – 3227, December 2004.

[9] W.H. Weedon, W.J. Payne, and G.M. Rebeiz, "MEMS-switched reconfigurable antennas" IEEE Antennas and Propagation Society International Symposium, Vol. 3, pp. 654 – 657, July 2001.

[10] C. E. Tong, and R. Blundel, "An annular slot antenna on a dielectric half-space", IEEE Transactions on Antennas and Propagation, Vol. 2, no.7, pp. 967 – 974, July 1994.

[11] S. Kanamaluru, Ming-Yi L, and Kai Chang, "Narrowband filter and annular slot antenna for PCS applications", IEEE MTT-S International Microwave Symposium Digest, Vol. 2 , pp. 987 – 990, June 1996.

[12] Cheng-Shong Hong, "Small annular slot antenna with capacitor loading" Electronics Letters , vol.36 , no.2, pp. 110 – 111, January 2000.

[13] K. Prasad, and L. Shafai, "'Higher order mode excitation in circular loop and annular slot antennas", IEEE Antennas and Propagation Society International Symposium, Vol. 25, pp. 824 – 827, Jun 1987.

[14] P. Mastin, B. Rawat and M., Williamson,"Design of a microstrip annular slot antenna for mobile communications" IEEE Antennas and Propagation Society International Symposium Digest. Held in Conjuction with: URSI Radio Science Meeting and Nuclear EMP Meeting, Vol. 1, pp. 507 – 510, July 1992.

[15] E. Irzinski, "The input admittance of a TEM excited annular slot antenna", IEEE Transactions on Antennas and Propagation, Vol. 23, Issue: 6, pp. 829 – 834, November 1975.

[16] N. Nikolic, J.S. Kot, and T.S. Bird, "Theoretical and experimental study of a cavity-backed annular-slot antenna", IEE Proceedings on Microwaves, Antennas and Propagation, Vol. 144, Issue: 5 , pp. 337 – 340, October 1997.

[17] Ming-Hau Yeh, Powen Hsu, and Jean-Fu Kiang, "Analysis of a CPW-fed slot ring antenna", Asia-Pacific Microwave Conference, Vol. 3, pp. 1267 - 1270 , December 2001.

[18] P. Minard, and A. Louzir, "A new wide frequency band feeding technique of annular slot antenna", IEEE Antennas and Propagation Society International Symposium, Vol. 1, pp. 406 – 409, June 2002.

[19] H. Tehrani and Kai Chang, "A multi-frequency microstrip-fed annular slot antenna", IEEE Antennas and Propagation Society International Symposium, Vol. 2, pp. 632 – 635, July 2000.

[20] F. Le Bolter, and A. Louzir, "Multi-band annular slot antenna for WLAN applications", IEEE Antennas and Propagation Society Conference, Vol. 2, pp. 529 – 532, April 2001.

[21] Quan Li, Zhongxiang Shen and Xiaoyong Shan, "A new microstrip-fed cavity-backed annular slot antenna", IEEE Antennas and Propagation Society International Symposium, Vol. 3, pp.68, June 2002.

[22] Young Hoon Suh and Ikmo Park, "A broadband eccentric annular slot antenna" IEEE Antennas and Propagation Society International Symposium, Vol. 1, pp. 94 – 97, July 2001.

[21] N. Behdad and K. Sarabandi, "A wideband bi-semicircular slot antenna", IEEE Antennas and Propagation Society Symposium, Vol.2, pp. 1903 – 1906, June 2004

[22] D.Peroulis, K. Sarabandi, L.P.B. Katehi, "Design of reconfigurable slot antennas", IEEE Transactions on Antennas and Propagation, Vol. 53, Issue 2, pp. 645 – 654, February 2005

[23] P. R. Urwin-Wright, G.S. Hilton, I. J. Craddock, and P. N. Fletcher, "An electrically-small annular slot operating in the 'DC' mode", Twelfth International Conference on Antennas and Propagation, Vol. 2, pp. 686 – 689, April 2003

[23] RongLin Li, G.DeJean, M.M. Tentzeris, and J. Laskar, "Development and analysis of a folded shorted-patch antenna with reduced size", IEEE Transactions on Antennas and Propagation, Vol. 52, Issue: 2, pp. 555 – 562, February 2004.

[24] P. Hallbjorner, "Electrically small unbalanced four-arm wire antenna" IEEE Transactions on Antennas and Propagation, Vol. 52, Issue: 6, pp. 1424 – 1428, June 2004.

[25] Ansoft HFSS

[26] C. A. Balanis, "Antenna Theory Analysis and Design", John Wiley & sons, Second Edition, pp. 152 –157.

[27] R. L. Li, V. F. Fusco and R. Cahil, "Pattern shaping using a reactively loaded wire loop antenna", IEE Proceedings on Microwaves, Antennas and Propagation, Vol. 148, Issue: 3, pp. 203 – 208, June 2004

[28] C.Lugo and J. Papapolymerou, “Electronic switchable bandpass filter using PIN diodes for wireless low cost system-on-a-package applications.” IEE Proceedings on Microwaves, Antennas and Propagation, Vol. 151, Issue: 6, pp. 497 – 502, December 2004.